International Journal of Engineering Research & Technology (IJERT)
ISSN: 2278-0181
Vol. 15 Issue 07 , July - 2026

Investigation of the Silicon Content of Sands from River Wudil for the Development of Solar PV Panel

Zainulabideen Abbati[1], Ali Hussain Ali[2], Hindatu Idris Umar[3], Yusuf Muhammad Sani[4]
[1] Department of Welding and Fabrication Engineering Technology, Kano State Polytechnic, Nigeria
[2] Department of Mechanical Engineering, Aliko Dangote University of Science and Technology Wudil, Nigeria
[,4]Department of Mechanical Engineering, Kano State Polytechnic, Nigeria
[3] Department of Textile and Polymer Technology, Kano State Polytechnic, Nigeria

Abstract - ***The increasing global demand for renewable energy has intensified the need for sustainable and locally available raw materials for photovoltaic (PV) technologies. Silicon, obtained primarily from silica (SiO_2), remains the principal semiconductor material used in the manufacture of crystalline solar photovoltaic cells due to its excellent electrical properties, abundance, and long-term stability. This study investigates the silicon content of River Wudil sand in Kano State, Nigeria, to evaluate its suitability as a potential raw material for silica extraction for the development of photovoltaic-related PVC solar panel components. Representative sand samples were collected from five different locations along River Wudil following standard sampling procedures. The samples were subjected to beneficiation processes, including washing, acid leaching, drying, magnetic separation, and sieve analysis before characterization using X-ray Fluorescence (XRF), Scanning Electron Microscopy (SEM), and Energy Dispersive X-ray Spectroscopy (EDX). The sieve analysis revealed that Samples C and D possessed well-graded medium-sized particles, making them more suitable for silica beneficiation due to their larger surface area and lower grinding requirements. XRF analysis showed that silicon dioxide (SiO_2) was the predominant oxide in all samples, with concentrations ranging from 75.92 wt.% to 79.60 wt.%, confirming that River Wudil sand is naturally rich in silica. However, impurities such as Al_2O_3, Fe_2O_3, K_2O, CaO, TiO_2, and trace metallic oxides were also detected, indicating that additional purification processes are required to achieve the high-purity silica needed for photovoltaic applications. SEM micrographs revealed predominantly sub-angular to sub-rounded quartz grains with relatively smooth surfaces, localized fractures, and limited impurity coatings, characteristics that favour efficient washing, acid leaching, and magnetic separation. Although the EDX results reported chromium and strontium as dominant detected elements, these findings were inconsistent with the XRF and SEM analyses due to the exclusion of oxygen during measurement, thereby limiting their reliability for quantitative elemental interpretation.***
Overall, the combined characterization results demonstrate that River Wudil sand possesses significant potential as a local silica resource for industrial beneficiation. Among the investigated samples, Sample A exhibited the highest silica content (79.60 wt.%), while Sample D contained the lowest concentrations of iron and titanium impurities, making these samples the most promising candidates for high-purity silica production after beneficiation. The study concludes that appropriate processing techniques, including washing, magnetic separation, milling, and acid leaching, can substantially improve the silica purity to meet the stringent requirements for advanced polymer composites and photovoltaic applications. The successful utilization of River Wudil silica would contribute to the development of indigenous raw materials for renewable energy technologies, reduce dependence on imported silica resources, lower manufacturing costs, and promote sustainable industrial development in Nigeria.

KEY WORDS; Silica Sand, PVC Panel, Solar, Renewable Energy, River Sand.

1. INTRODUCTION

The rapid increase in global energy demand, coupled with growing environmental concerns associated with the extensive use of fossil fuels, has accelerated the transition towards renewable energy technologies. Conventional energy sources such as coal, crude oil, and natural gas remain the dominant contributors to global electricity generation; however, their continuous utilization has resulted in significant greenhouse gas emissions, climate change, environmental degradation, and depletion of finite natural resources. Consequently, governments, industries, and research institutions across the world are investing heavily in sustainable energy systems capable of providing clean, affordable, and reliable electricity while minimizing environmental impacts. Among the various renewable energy technologies currently available, solar photovoltaic (PV) systems have emerged as one of the most promising solutions because of their abundance, scalability, low operating costs, and ability to generate electricity directly from sunlight without producing harmful emissions during operation [1], [2].

International Journal of Engineering Research & Technology (IJERT)
ISSN: 2278-0181
Vol. 15 Issue 07 , July - 2026

The deployment of solar photovoltaic technology has experienced unprecedented growth over the past two decades owing to continuous improvements in conversion efficiency, reductions in manufacturing costs, supportive government policies, and increasing public awareness regarding environmental sustainability. According to the International Energy Agency (IEA), solar PV has become the fastest-growing renewable electricity technology worldwide, accounting for a significant proportion of newly installed renewable energy capacity in recent years. Global installed photovoltaic capacity surpassed one terawatt (TW), and projections indicate that the capacity may exceed 14 TW by 2050 to achieve international carbon neutrality targets and satisfy the rapidly growing electricity demand [1], [3]. Similarly, the International Renewable Energy Agency (IRENA) reports that renewable energy installations continue to expand annually, with solar PV contributing the largest share of newly installed renewable capacity because of its declining levelized cost of electricity and technological maturity [2].

The remarkable expansion of the photovoltaic industry has inevitably resulted in a corresponding increase in the demand for high-quality raw materials required for manufacturing solar cells and associated photovoltaic components. Silicon remains the dominant semiconductor material used in crystalline photovoltaic technologies, accounting for more than 95% of commercially manufactured solar cells worldwide [4]. This dominance is attributable to silicon's excellent semiconductor properties, suitable electronic band gap, high thermal stability, mechanical strength, long operational lifetime, and the abundance of silicon-containing minerals within the Earth's crust. Crystalline silicon photovoltaic cells also exhibit relatively high conversion efficiencies compared with alternative thin-film technologies while maintaining excellent durability under varying environmental conditions [5].

Silicon is the second most abundant element in the Earth's crust after oxygen, constituting approximately 27–28% of the crustal composition by mass. However, elemental silicon does not occur naturally because of its high chemical affinity for oxygen. Instead, it exists predominantly in the form of silicon dioxide (SiO_2) and various silicate minerals present in igneous, metamorphic, and sedimentary rocks [6]. Quartz, quartzite, sandstone, and silica-rich river sands represent the principal naturally occurring sources of silicon dioxide exploited for industrial applications. Industrial silicon production generally involves the carbothermic reduction of silica in electric arc furnaces operating at temperatures exceeding 2,000°C to produce metallurgical-grade silicon. Subsequent purification processes such as chemical vapor deposition and zone refining are employed to obtain electronic-grade or solar-grade silicon suitable for photovoltaic cell fabrication [7].

The quality of silica feedstock plays a critical role in determining the efficiency, purity, and economic viability of silicon production. High-purity silica is an essential raw material not only for photovoltaic cells but also for glass manufacturing, semiconductor devices, optical fibres, ceramics, refractories, silicone chemicals, advanced composites, and numerous engineering applications [8]. For photovoltaic manufacturing, silica feedstock must possess exceptionally high silicon dioxide content while containing very low concentrations of metallic impurities such as iron, titanium, aluminium, calcium, sodium, potassium, and magnesium. These impurities can adversely affect the electrical, optical, and mechanical properties of silicon by introducing undesirable defects during crystal growth and semiconductor processing [9].

Natural silica sands vary considerably in mineralogical composition depending on their geological origin, transportation history, depositional environment, and weathering processes. River sands are particularly attractive as potential silica resources because continuous hydraulic transportation promotes natural washing, sorting, and concentration of resistant quartz minerals while removing softer and less stable mineral constituents. Nevertheless, even silica-rich river sands usually contain appreciable quantities of feldspars, clay minerals, iron oxides, heavy minerals, carbonates, and organic matter that must be removed through beneficiation processes before the silica becomes suitable for high-value industrial applications [10].

Beneficiation refers to a combination of physical and chemical treatment processes employed to improve the purity of mineral resources by removing undesirable impurities. For silica sand, commonly adopted beneficiation techniques include washing, attrition scrubbing, magnetic separation, gravity concentration, flotation, sieving, milling, and acid leaching. Physical separation techniques eliminate coarse particles, clay minerals, and magnetic contaminants, whereas chemical treatments dissolve metallic oxides and carbonate impurities that remain attached

International Journal of Engineering Research & Technology (IJERT)
ISSN: 2278-0181
Vol. 15 Issue 07 , July - 2026

to quartz grain surfaces [11]. Acid leaching using hydrochloric acid (HCl), sulfuric acid (H_2SO_4), oxalic acid, hydrofluoric acid (HF), or combinations thereof has been widely reported as one of the most effective methods for reducing iron, aluminium, titanium, and alkali impurities to levels acceptable for advanced industrial applications [12].

The characterization of silica-bearing materials before and after beneficiation is equally important because it provides detailed information regarding chemical composition, mineralogy, particle morphology, surface texture, elemental distribution, and impurity concentrations. Modern analytical techniques such as X-ray Fluorescence (XRF), X-ray Diffraction (XRD), Scanning Electron Microscopy (SEM), Energy Dispersive X-ray Spectroscopy (EDX), Fourier Transform Infrared Spectroscopy (FTIR), and Inductively Coupled Plasma Optical Emission Spectroscopy (ICP-OES) are routinely employed to evaluate silica resources intended for industrial processing [13]. Among these methods, XRF provides reliable quantitative information on the bulk oxide composition of silica sand, SEM reveals particle morphology and surface characteristics, while EDX complements SEM observations by identifying localized elemental distributions on mineral surfaces [14].

Particle size distribution constitutes another important factor influencing the efficiency of silica beneficiation and extraction. Fine and uniformly graded particles generally provide larger specific surface areas that enhance acid penetration and impurity dissolution during chemical treatment. Conversely, excessively coarse particles require additional crushing and milling, thereby increasing energy consumption and processing costs. Consequently, sieve analysis is routinely performed before beneficiation to determine the optimum processing conditions required for maximizing silica recovery and minimizing operational expenses [15].

Growing industrialization and increasing demand for photovoltaic materials have intensified the search for alternative indigenous silica resources capable of reducing dependence on imported raw materials. Many developing countries possess abundant silica deposits that remain underutilized because of limited characterization and insufficient beneficiation research. Nigeria is endowed with significant deposits of silica-rich sands distributed across river channels, flood plains, coastal environments, and sedimentary basins. Previous investigations have identified commercially promising silica deposits in several states, including Ogun, Delta, Kaduna, Plateau, Kogi, Cross River, and Kano. However, many of these deposits have not been comprehensively evaluated regarding their suitability for photovoltaic and other high-technology applications [16], [17].

The utilization of locally available silica resources presents substantial economic and technological advantages for Nigeria. Domestic production of high-purity silica could stimulate local manufacturing of photovoltaic components, reduce foreign exchange expenditure associated with raw material importation, create employment opportunities, promote technology transfer, and support national renewable energy development policies. Furthermore, developing indigenous silica beneficiation technologies would contribute significantly to achieving the country's industrialization objectives and sustainable development goals through increased value addition to locally available mineral resources [18].

The quality of silica required for photovoltaic applications is considerably higher than that required for conventional industrial uses such as construction, foundry moulds, and glass production. While ordinary industrial silica sand may contain between 90 and 98 wt.% SiO_2, the production of metallurgical-grade silicon and, ultimately, solar-grade silicon demands feedstock with exceptionally low concentrations of metallic impurities. Iron, aluminium, titanium, calcium, magnesium, potassium, sodium, and other trace elements must be reduced to very low levels because even minute concentrations can adversely affect the electrical characteristics of silicon wafers by introducing recombination centres, reducing carrier lifetime, and lowering photovoltaic conversion efficiency [19], [20]. Consequently, the successful production of high-quality photovoltaic materials depends not only on the abundance of silica but also on the effectiveness of purification and beneficiation processes capable of producing feedstock that satisfies stringent industrial specifications.

Recent advances in mineral processing have demonstrated that naturally occurring silica sands containing moderate impurity concentrations can be upgraded into high-purity silica suitable for advanced industrial applications through carefully designed beneficiation routes. Mechanical processing techniques such as washing, screening, attrition scrubbing, gravity concentration, and magnetic separation are frequently employed as

International Journal of Engineering Research & Technology (IJERT)
ISSN: 2278-0181
Vol. 15 Issue 07 , July - 2026

preliminary operations to remove clay minerals, organic matter, and iron-bearing heavy minerals from raw silica sand. These methods are often followed by chemical treatments, particularly acid leaching, which selectively dissolves metallic contaminants remaining on the quartz grain surfaces while preserving the chemically stable silica matrix [21]. The effectiveness of these treatments depends on several factors, including particle size distribution, mineralogical composition, acid concentration, reaction temperature, leaching duration, and the nature of impurity associations within the quartz grains [22].

Hydrochloric acid (HCl) is widely used for the removal of carbonates, iron oxides, and alkali-bearing minerals because of its strong dissolving ability and relatively low environmental impact compared with certain alternative mineral acids. Hydrofluoric acid (HF), although highly hazardous and requiring stringent safety precautions, has also been employed for the dissolution of silicate impurities and the removal of surface contamination from quartz particles. Other researchers have reported successful purification using sulfuric acid, nitric acid, oxalic acid, citric acid, and mixed-acid systems depending on the mineralogical characteristics of the silica deposit under investigation [23]. The selection of an appropriate beneficiation strategy therefore requires a comprehensive understanding of the chemical and morphological characteristics of the raw material before processing.

Characterization techniques have consequently become indispensable tools in silica beneficiation studies because they provide scientific evidence regarding the suitability of a deposit for industrial utilization. X-ray Fluorescence (XRF) spectroscopy is widely recognized as one of the most reliable techniques for determining the bulk chemical composition of silica-bearing materials. The technique provides quantitative information on the concentration of major and trace oxides, enabling researchers to assess silica purity and identify the principal contaminants requiring removal during beneficiation [24]. Since silica extraction is fundamentally influenced by the concentration of silicon dioxide and associated impurities, XRF analysis forms the basis for evaluating the industrial potential of natural silica deposits.

Scanning Electron Microscopy (SEM) complements chemical characterization by providing high-resolution images of particle morphology, grain shape, surface texture, fractures, and impurity coatings. The morphology of quartz grains influences washing efficiency, acid accessibility, and mechanical processing behaviour. Quartz particles possessing sub-angular to sub-rounded shapes with limited surface contamination generally exhibit improved beneficiation characteristics because impurities are concentrated primarily on grain surfaces rather than being incorporated into the crystal lattice [25]. Surface fractures and micro-cracks observed under SEM further enhance chemical purification by increasing the available surface area for acid penetration and impurity dissolution.

Energy Dispersive X-ray Spectroscopy (EDX), when integrated with SEM, provides localized elemental information from selected regions of the specimen. Unlike XRF, which analyses the bulk composition of the sample, EDX examines comparatively small areas and is therefore particularly useful for identifying surface contaminants, localized mineral inclusions, and the elemental distribution associated with individual grains. Nevertheless, the interpretation of EDX data requires careful consideration of instrument operating conditions, detector settings, and analytical limitations because the omission of critical elements or inappropriate calibration parameters may produce misleading quantitative results [26]. Consequently, meaningful mineralogical interpretation is generally achieved by integrating SEM observations with XRF chemical analysis and other complementary characterization techniques.

Particle size distribution also plays a significant role in determining beneficiation efficiency and overall silica recovery. Quartz particles with relatively uniform sizes promote effective washing, improve magnetic separation efficiency, and facilitate homogeneous acid penetration during chemical treatment. Conversely, highly heterogeneous particle size distributions may result in uneven purification, increased reagent consumption, and additional comminution requirements. Sieve analysis therefore provides valuable information for selecting suitable processing conditions while minimizing energy consumption and production costs [27]. In industrial mineral processing, optimized particle size not only enhances beneficiation performance but also improves the quality and consistency of the final silica product used in polymer composites, glass manufacturing, and photovoltaic applications.

International Journal of Engineering Research & Technology (IJERT)
ISSN: 2278-0181
Vol. 15 Issue 07 , July - 2026

Apart from its application in crystalline silicon solar cells, purified silica has gained increasing importance as a functional engineering material in polymer-based photovoltaic systems. Polyvinyl chloride (PVC) remains one of the most widely used thermoplastic polymers because of its low cost, ease of fabrication, chemical resistance, and excellent weathering characteristics. However, the incorporation of mineral fillers such as high-purity silica significantly enhances the mechanical strength, stiffness, abrasion resistance, thermal stability, dimensional stability, ultraviolet resistance, and long-term durability of PVC composites used in outdoor environments [28]. The performance improvements achieved through silica reinforcement have encouraged researchers to investigate locally available silica resources capable of supporting the manufacture of high-performance polymer composites for renewable energy applications.

The development of photovoltaic support structures, encapsulation materials, electrical insulation components, cable protection systems, mounting accessories, and protective polymeric housings increasingly relies on advanced composite materials incorporating finely dispersed silica fillers. Consequently, the availability of locally sourced high-purity silica presents substantial opportunities for reducing manufacturing costs while simultaneously promoting domestic industrial development. Countries possessing abundant silica resources can therefore establish integrated value chains linking mineral extraction, beneficiation, materials processing, and renewable energy manufacturing, thereby reducing dependence on imported industrial raw materials [29].

Nigeria possesses extensive geological formations containing quartz-rich sands distributed across river systems, sedimentary basins, coastal environments, and weathered granitic terrains. Numerous investigations have reported significant silica occurrences in states such as Ogun, Kaduna, Plateau, Kogi, Cross River, Delta, Edo, and Kano. Despite these abundant resources, the majority of silica utilized in high-value industrial applications continues to be imported because many local deposits have not undergone detailed physicochemical characterization or systematic beneficiation studies [30]. The limited availability of comprehensive scientific data concerning the purity, morphology, mineralogical composition, and beneficiation behaviour of many Nigerian silica deposits has consequently restricted their industrial exploitation.

River Wudil, located within Kano State in northwestern Nigeria, represents one such underexplored silica resource. Continuous fluvial transportation and sediment deposition have resulted in the accumulation of quartz-rich sands that may constitute an economically viable source of silica for advanced industrial applications. However, the suitability of these deposits for photovoltaic-related applications depends on several critical factors, including silica concentration, impurity levels, particle size distribution, grain morphology, and the effectiveness of beneficiation processes. Existing literature provides very limited information regarding the physicochemical characteristics of River Wudil sand, particularly with respect to its potential as a feedstock for high-purity silica production. This knowledge gap limits informed decision-making concerning its industrial utilization and underscores the need for comprehensive scientific investigation.

Accordingly, the present study investigates the silicon content and silica potential of River Wudil sand through an integrated experimental approach involving standardized sampling, beneficiation, particle size analysis, X-ray Fluorescence (XRF), Scanning Electron Microscopy (SEM), and Energy Dispersive X-ray Spectroscopy (EDX). The combined use of these analytical techniques provides comprehensive information regarding the chemical composition, particle morphology, elemental distribution, and impurity characteristics of the investigated samples. Such information is essential for evaluating the feasibility of upgrading River Wudil sand into high-purity silica suitable for photovoltaic-related applications and advanced polymer composite manufacturing.

Unlike previous studies that have focused primarily on identifying silica deposits or reporting basic chemical compositions, this research integrates particle size characterization with complementary chemical and microstructural analyses to establish the beneficiation potential of River Wudil sand. Furthermore, the study evaluates the relationship between silica content, impurity distribution, and processing requirements, thereby providing practical guidance for future large-scale silica purification and industrial utilization. The findings are expected to contribute to the growing body of knowledge on indigenous mineral resource development while supporting Nigeria's transition toward sustainable renewable energy technologies, local content development, and value-added mineral processing.

International Journal of Engineering Research & Technology (IJERT)
ISSN: 2278-0181
Vol. 15 Issue 07 , July - 2026

Ultimately, the successful utilization of River Wudil silica would provide multiple socioeconomic and technological benefits, including reduced dependence on imported silica feedstock, lower manufacturing costs for photovoltaic-related materials, enhanced utilization of indigenous mineral resources, employment generation within the mining and manufacturing sectors, and strengthened capacity for domestic renewable energy production. These anticipated outcomes align closely with national industrialization strategies, sustainable development objectives, and global efforts to accelerate the transition toward cleaner and more resilient energy systems. Against this background, the present investigation seeks to evaluate the suitability of River Wudil sand as a potential source of silica for the development of photovoltaic-related PVC composite materials through detailed physicochemical characterization and beneficiation assessment [31], [32].

RESEARCH GAP

Despite the increasing global demand for high-purity silica as a precursor for photovoltaic (PV) materials and advanced polymer composites, research on the characterization and beneficiation of indigenous silica resources in Nigeria remains limited. Numerous studies have focused on the extraction of silica from quartz, beach sands, and industrial silica deposits in different parts of the world; however, relatively few investigations have comprehensively evaluated river sand deposits in northern Nigeria for photovoltaic-related applications. Most existing studies have primarily reported the chemical composition of silica sand without integrating detailed particle size analysis, microstructural characterization, and elemental analysis required to assess the beneficiation potential of the material.

Previous investigations on Nigerian silica deposits have largely concentrated on glass manufacturing, foundry applications, ceramics, and construction materials, with limited attention given to their suitability as raw materials for photovoltaic technologies or polymer-based solar panel components. In addition, many published studies have relied solely on X-ray Fluorescence (XRF) analysis to determine silica content, while neglecting complementary characterization techniques such as Scanning Electron Microscopy (SEM) and Energy Dispersive X-ray Spectroscopy (EDX), which provide critical information on particle morphology, surface characteristics, impurity distribution, and elemental composition. Consequently, the relationships between particle morphology, impurity occurrence, beneficiation efficiency, and the potential utilization of silica in photovoltaic applications remain insufficiently understood.

Furthermore, although several silica-rich deposits have been identified across Nigeria, there is a paucity of scientific information regarding the physicochemical properties of River Wudil sand in Kano State. Specifically, there is limited published literature addressing its silicon dioxide content, impurity profile, grain size distribution, mineralogical characteristics, and suitability for producing high-purity silica required for photovoltaic-related applications. The absence of such information has hindered the development and industrial utilization of this potentially valuable indigenous mineral resource.

Another significant gap in the literature is the lack of integrated studies that combine beneficiation processes with comprehensive material characterization to determine the feasibility of upgrading naturally occurring river sand into silica suitable for renewable energy applications. Most available studies evaluate either beneficiation efficiency or material characterization independently, without establishing a clear relationship between particle size, chemical composition, surface morphology, impurity distribution, and the expected performance of the purified silica in photovoltaic materials. This fragmented approach limits the practical application of research findings for industrial-scale silica production.

Moreover, increasing global efforts to localize raw material supply chains for renewable energy technologies have highlighted the importance of developing indigenous mineral resources. However, there remains insufficient information on the potential contribution of locally sourced silica from River Wudil to Nigeria's renewable energy sector, particularly regarding its use as a reinforcing filler in PVC composites and as a precursor for high-purity silica production. Addressing these gaps is essential for promoting local content development, reducing dependence on imported silica materials, and supporting sustainable industrialization within the country.

Therefore, this study seeks to bridge these knowledge gaps through a comprehensive investigation of River Wudil sand using standardized sampling procedures, beneficiation techniques, sieve analysis, XRF, SEM, and EDX characterization. The study provides an integrated evaluation of the chemical composition, particle morphology,

International Journal of Engineering Research & Technology (IJERT)
ISSN: 2278-0181
Vol. 15 Issue 07 , July - 2026

elemental distribution, and beneficiation potential of the sand, thereby generating scientific data required to determine its suitability as a local source of silica for photovoltaic-related PVC solar panel manufacturing.

NOVELTY OF THE STUDY

The novelty of this research lies in its comprehensive and integrated evaluation of River Wudil sand as a potential indigenous source of silica for photovoltaic-related applications, an area that has received little or no detailed scientific investigation. Unlike previous studies that primarily focused on the chemical composition of silica deposits for conventional industrial uses, this study combines particle size analysis, beneficiation processes, X-ray Fluorescence (XRF), Scanning Electron Microscopy (SEM), and Energy Dispersive X-ray Spectroscopy (EDX) to provide a holistic assessment of the suitability of River Wudil sand for high-purity silica production.

A major contribution of this work is the establishment of a direct relationship between particle size distribution, chemical composition, microstructural characteristics, and beneficiation potential. By integrating sieve analysis with advanced physicochemical characterization, the study demonstrates how particle morphology and impurity distribution influence silica purification efficiency and the overall suitability of the material for photovoltaic applications. This multidisciplinary approach provides a more comprehensive understanding of the material than studies relying solely on chemical analysis.

Another novel aspect of this research is the evaluation of River Wudil sand specifically for photovoltaic-related PVC solar panel applications rather than traditional applications such as glassmaking, ceramics, or foundry production. The study therefore extends the potential utilization of Nigerian silica resources into the rapidly expanding renewable energy sector, contributing to the growing body of knowledge on sustainable materials for solar energy technologies.

Furthermore, the study critically compares the results obtained from XRF, SEM, and EDX analyses to assess the reliability of each characterization technique. The identification and discussion of inconsistencies observed in the EDX results, together with their correlation to XRF and SEM findings, provide valuable methodological insights for future researchers undertaking similar investigations on silica-bearing materials.

The research also provides one of the first comprehensive datasets on the physicochemical characteristics of River Wudil sand, including its silicon dioxide concentration, impurity profile, grain morphology, particle size distribution, and beneficiation requirements. These baseline data constitute an important scientific resource for future investigations into silica purification, solar-grade silicon production, polymer composite development, and other advanced industrial applications.

Finally, this study contributes to the broader objective of promoting sustainable utilization of indigenous mineral resources by demonstrating the feasibility of converting an underutilized natural river sand deposit into a value-added industrial raw material. The findings have significant implications for reducing dependence on imported silica, supporting local manufacturing of photovoltaic materials, enhancing mineral resource utilization, and advancing Nigeria's renewable energy and industrial development agenda. The integrated methodology and comprehensive characterization framework presented in this research may also serve as a reference model for evaluating similar silica deposits in other regions of Nigeria and beyond.

2.0 MATERIALS AND METHODS

2.1 Study Area Description

Wudil is located in Kano State, Nigeria, within latitude 11.79°N–11.81°N and longitude 8.83°E–8.84°E. The area lies within the Sudan savannah zone and is influenced by semi-arid climatic conditions. River Wudil forms part of the Hadejia River basin and contributes to sediment deposition suitable for silica investigation.

2.2 Materials

1) The materials used in this study include;

- Wudil River sand samples, Hydrofluoric acid (HF), Hydrochloric acid (HCl), Distilled water and Tap water.

2) Equipment

The following equipment were used for the experimentation;

- 250 mL conical flasks, 50 mL measuring cylinders, Mechanical stirrer, 4 L plastic, Specimen discs, washing container, Laboratory oven, Bar magnet, Standard sieve set, (XRF analyzer, SEM and EDX equipment located

International Journal of Engineering Research & Technology (IJERT)
ISSN: 2278-0181
Vol. 15 Issue 07 , July - 2026

at Olanrewaju Gabriel Department of Mechanical engineering, Covenant University, Canaan land, sango OTA, Ogun state)

2.3 Methods

2.3.1 Sample Collection

Samples were collected from five different locations using ASTM D75/D75M.

Sand samples were collected from five (5) different locations along River Wudil to ensure representativeness.

Procedure:

1. Sampling points were selected at intervals along the river (upstream, midstream, downstream, and two intermediate points).
2. At each location, sand was collected from a depth of 10–30 cm using a clean stainless-steel scoop.
3. Approximately 2 kg of sand was collected per location.
4. Samples were stored in labeled polyethylene bags.

Plate 1. Deposit of Sand in River wudil as Selected Area.

2.3.2 Pretreatment (Leaching)

Samples were treated with HCl and HF following ASTM D3875.

The sand samples were purified using acid leaching to remove impurities such as iron oxides and carbonates.

Procedure:

1. Samples were washed with distilled water to remove clay and organic matter.
2. The cleaned sand was dried and then treated with:

Hydrochloric acid (HCl) to remove carbonates and metal impurities.

Hydrofluoric acid (HF) to dissolve silicate impurities.

3. The mixture was stirred and allowed to react for 2–4 hours.
4. The treated samples were thoroughly rinsed with distilled water until neutral pH was achieved.

2.3.3 Drying

Samples were dried at 105°C using ASTM C566.

After leaching, samples were dried to remove moisture.

Procedure:

1. The washed samples were placed in a laboratory oven.
2. Drying was carried out at 105°C ± 5°C for 24 hours.
3. Samples were cooled in a desiccator.

International Journal of Engineering Research & Technology (IJERT)
ISSN: 2278-0181
Vol. 15 Issue 07 , July - 2026

Plate 2. Sand sample under Oven dried

2.3.4 Magnetic Separation

Magnetic particles were removed using ASTM A342.
Magnetic separation was carried out to remove iron-bearing minerals.
Procedure:
1. Dried samples were spread on a clean surface.
2. A bar magnet was passed repeatedly over the sample.
3. Magnetic particles (e.g., iron filings) were removed.
4. The process was repeated until no further magnetic particles were detected.

Plate 3. Sand sample Undergoing magnetization.

2.3.5 Sieve Analysis

Particle size distribution determined using ASTM C136.
Particle size distribution was determined using sieve analysis.
Procedure:
1. A representative sample (~500 g) was obtained.
2. The sample was placed in a stack of standard sieves arranged in descending order.
3. The sieve shaker was operated for 10–15 minutes.
4. The mass retained on each sieve was recorded.

International Journal of Engineering Research & Technology (IJERT)
ISSN: 2278-0181
Vol. 15 Issue 07 , July - 2026

Plate 4. Sand sample undergoing sieve analysis.

2.3.6 XRF Analysis

Sand sample Chemical analysis (XRF, EDX and SEM) was conducted at the chemical analysis laboratory located at Olanrewaju Gabriel Department of Mechanical engineering, Covenant University, Canaan land, sango OTA, Ogun state).

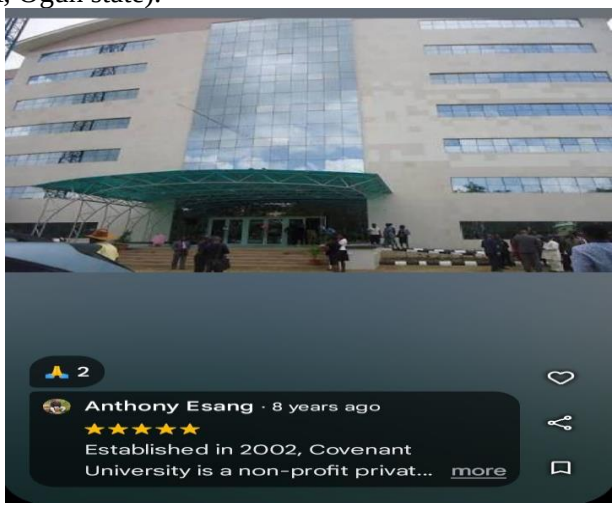

Plate 5. Location for sand sample chemical analysis.

Chemical composition determined using ASTM C114.
XRF analysis was used to determine the elemental composition, especially silica (SiO_2).
Procedure:
1. The sample was ground into fine powder (<75 µm).
2. Pellets were prepared using a hydraulic press.
3. The sample was analyzed using an XRF spectrometer.
4. The percentage composition of SiO_2 and other oxides was recorded

2.3.7 EDX Analysis

Elemental analysis conducted using ASTM E1508.
EDX analysis was used to confirm elemental composition.
Procedure:
1. A small quantity of the sample was mounted on a sample holder.
2. The sample was coated with conductive material (if required).
3. The EDX system attached to SEM was used to analyze elemental composition.

2.3.8 SEM Analysis

International Journal of Engineering Research & Technology (IJERT)
ISSN: 2278-0181
Vol. 15 Issue 07 , July - 2026

Surface morphology studied using ASTM E986.
SEM was used to study the morphology and surface characteristics of the sand particles.
Procedure:
1. Samples were mounted on SEM stubs.
2. The sample surface was coated with gold or carbon.
3. Imaging was carried out at magnifications.
4. Micrographs were obtained to observe particle shape and texture.

3. Characterizations.

3.1 Sieving Analysis

The grain size distribution analysis, performed using a set of standard sieves, revealed that the sieve analysis presents the particle size distribution of five sand samples (A–E) with an initial weight of **1000 g** each. The final recovered weights (992 g, 980 g, 872 g, 996 g, and 842 g) indicate minor to moderate material losses during sieving, with Samples C and E showing the greatest losses, possibly due to dust, handling losses, or the presence of very fine particles.

Sample Initial weight = 1000g

Sample No.	A	B	C	D	E
Final	992	980	872	996	842
600	76	40	26	34	80
425	48	38	38	42	46
300	16	26	32	32	16
212	6	10	20	8	4
150	2	24	26	26	2
63	2	12	8	8	2

3.1.1 Particle Size Distribution

The sieve sizes are **600, 425, 300, 212, 150, and 63 µm**. The results indicate the following trends:

Sample	Dominant Particle Size	Interpretation
A	600 µm (76%)	Very coarse sand
B	600 µm (40%) and 425 µm (38%)	Moderately coarse with good grading
C	425 µm (38%), 300 µm (32%), 150 µm (26%)	Well-distributed medium sand
D	425 µm (42%) and 300 µm (32%)	Uniform medium-coarse sand
E	600 µm (80%)	Extremely coarse sand

The majority of particles in Samples **A** and **E** are retained on the **600 µm sieve**, indicating coarse-grained sand. Samples **C** and **D** exhibit a more balanced distribution across the 425–150 µm size range, suggesting better grading.

3.1.2 Implications for Silica Extraction

Particle size plays an important role in silica extraction because it influences:

- Surface area available for chemical reactions.
- Efficiency of washing and impurity removal.
- Grinding energy required before purification.
- Consistency during processing.

Sample A

- Predominantly coarse particles (600 µm).
- Requires additional crushing or milling before chemical purification.
- Lower surface area reduces reaction efficiency during leaching.

Sample B

- Good balance between coarse and medium particles.
- Easier to process than Sample A.
- Suitable for beneficiation with moderate grinding.

International Journal of Engineering Research & Technology (IJERT)
ISSN: 2278-0181
Vol. 15 Issue 07 , July - 2026

Sample C

- Well-graded distribution.
- Higher proportion of medium-sized particles.
- Offers larger surface area for acid leaching.
- Likely to achieve higher silica recovery with lower energy consumption.

Sample D

- Similar to Sample C but slightly coarser.
- Suitable feedstock after washing and classification.
- Expected to produce high-purity silica efficiently.

Sample E

- Very coarse material.
- Significant size reduction required.
- Highest grinding cost before purification.

3.1.3 Suitability for PVC Solar Panel Manufacturing

For PVC solar panel production, silica is generally used as:

- A reinforcing filler.
- A functional additive to improve mechanical strength.
- A UV-resistant additive after purification.
- A raw material for producing high-purity silica powders.

Manufacturers generally prefer silica with:

- High SiO_2 purity (typically above **98–99%**, depending on the application).
- Uniform particle size.
- Low iron content.
- Low clay and organic impurities.
- Fine particle size after milling (often below **75–100 µm** for filler applications).

The sieve analysis only provides information about **particle size**, not chemical composition. Therefore, it cannot by itself confirm that the sand is suitable for PVC solar panel manufacturing. Chemical analyses such as:

- X-ray fluorescence (XRF),
- X-ray diffraction (XRD),
- ICP-OES,
- or wet chemical analysis are necessary to determine silica purity and impurity levels.

3.1.4 Best Sample Based on the Sieving Results

Considering particle size alone:

1. **Sample C** – Most suitable due to its well-graded medium-sized particles, which require less grinding and offer better processing efficiency.
2. **Sample D** – Also suitable with a relatively uniform distribution.
3. **Sample B** – Acceptable but contains more coarse particles.
4. **Sample A** – Requires significant milling before silica extraction.
5. **Sample E** – Least suitable because of its predominantly coarse particle size and higher expected processing cost.

3.2 Chemical Composition

The X-ray Fluorescence (XRF) analysis was conducted to determine the chemical composition of five Wudil River sand samples (A–E). The results show that **silicon dioxide (SiO_2)** is the dominant oxide in all samples, confirming that the river sand is principally siliceous and has good potential as a raw material for silica extraction. However, the presence of impurities such as **Al_2O_3, Fe_2O_3, K_2O, CaO, TiO_2, and Cl** indicates that beneficiation and purification processes will be necessary before the silica can be used in high-quality PVC solar panel applications.

Analysis Report for Sand Sample A

International Journal of Engineering Research & Technology (IJERT)
ISSN: 2278-0181
Vol. 15 Issue 07 , July - 2026

Thick	Type	Error	Units	Density	Norm.	Total
1 0.00	Bulk	0.00	mg/cm2	0.00F	On	100.00

Sample Table

Layer	Component	Type	Concn.	Error	Units	Mole%	Error
1	SiO2	Calc	79.602	1.917	wt.%	84.955	2.046
1	V2O5	Calc	0.126	0.019	wt.%	0.044	0.007
1	Cr2O3	Calc	0.003	0.010	wt.%	0.001	0.004
1	MnO	Calc	0.038	0.009	wt.%	0.034	0.008
1	Fe2O3	Calc	1.405	0.027	wt.%	0.564	0.011
1	CoO	Calc	0.013	0.009	wt.%	0.011	0.008
1	NiO	Calc	0.002	0.006	wt.%	0.001	0.005
1	CuO	Calc	0.067	0.006	wt.%	0.054	0.005
1	Nb2O5	Calc	0.025	0.008	wt.%	0.006	0.002
1	WO3	Calc	0.000	0.000	wt.%	0.000	0.000
1	P2O5	Calc	0.000	0.000	wt.%	0.000	0.000
1	SO3	Calc	0.780	0.153	wt.%	0.625	0.123
1	CaO	Calc	1.025	0.073	wt.%	1.173	0.084
1	MgO	Calc	0.000	0.000	wt.%	0.000	0.000
1	K2O	Calc	6.902	0.177	wt.%	4.698	0.121
1	BaO	Calc	0.158	0.118	wt.%	0.066	0.049
1	Al2O3	Calc	6.807	3.621	wt.%	4.281	2.277
1	Ta2O5	Calc	0.084	0.022	wt.%	0.012	0.003
1	TiO2	Calc	1.229	0.046	wt.%	0.987	0.037
1	ZnO	Calc	0.001	0.004	wt.%	0.001	0.003
1	Ag2O	Calc	0.025	0.050	wt.%	0.007	0.014
1	Cl	Calc	1.273	0.089	wt.%	2.302	0.162
1	ZrO2	Calc	0.037	0.007	wt.%	0.019	0.004
1	SnO2	Calc	0.241	0.539	wt.%	0.103	0.229
1	PbO	Calc	0.025	0.012	wt.%	0.007	0.004
1	Rb2O	Calc	0.031	0.005	wt.%	0.011	0.002
1	Cs2O	Calc	0.069	0.123	wt.%	0.016	0.028
1	SrO	Calc	0.031	0.006	wt.%	0.019	0.003

Element Table

Elmt	Line	Cond	Ratio	Intensity	Error	Intensity	Conc.	Conc	Calibration	Coefficient
Code	Code			(c/s)	(c/s)	Method		Method		
O	Ka	0	None	0.000	0.0000	Gaussian	48.640	None		0.000
Mg	Ka	1	None	0.000	3.6320	Gaussian	0.000	FP		0.000
Al	Ka	1	None	22.846	12.1536	Gaussian	3.603	FP		0.000
Si	Ka	1	None	1210.444	29.1579	Gaussian	37.210	FP		0.000
P	Ka	1	None	0.000	15.3952	Gaussian	0.000	FP		0.000
S	Ka	1	None	34.974	6.8671	Gaussian	0.313	FP		0.000
Cl	Ka	1	None	189.170	13.2756	Gaussian	1.273	FP		0.000
K	Ka	1	None	1269.197	32.5814	Gaussian	5.729	FP		0.000
Ca	Ka	1	None	217.929	15.5326	Gaussian	0.733	FP		0.000
Ti	Ka	1	None	485.044	18.1273	Gaussian	0.737	FP		0.000
V	Ka	1	None	63.339	9.6407	Gaussian	0.070	FP		0.000

International Journal of Engineering Research & Technology (IJERT)
ISSN: 2278-0181
Vol. 15 Issue 07 , July - 2026

Cr	Ka	1	None	2.132	8.2322	Gaussian	0.002	FP	0.000
Mn	Ka	1	None	42.798	9.7707	Gaussian	0.029	FP	0.000
Fe	Ka	1	None	1749.874	34.1365	Gaussian	0.983	FP	0.000
Co	Ka	1	None	22.511	14.9771	Gaussian	0.011	FP	0.000
Ni	Ka	1	None	3.215	10.8060	Gaussian	0.001	FP	0.000
Cu	Ka	1	None	148.741	13.4615	Gaussian	0.054	FP	0.000
Zn	Ka	1	None	1.824	10.5404	Gaussian	0.001	FP	0.000
Rb	Ka	1	None	103.725	15.4551	Gaussian	0.028	FP	0.000
Sr	Ka	1	None	86.168	15.2190	Gaussian	0.027	FP	0.000
Zr	Ka	1	None	76.360	14.8877	Gaussian	0.028	FP	0.000
Nb	Ka	1	None	42.506	14.2832	Gaussian	0.017	FP	0.000
Ag	Ka	1	None	5.474	10.9853	Gaussian	0.023	FP	0.000
Sn	La	1	None	13.472	30.0814	Gaussian	0.190	FP	0.000
Cs	La	1	None	9.144	16.3360	Gaussian	0.065	FP	0.000
Ba	La	1	None	22.980	17.1771	Gaussian	0.141	FP	0.000
Ta	La	1	None	52.350	14.0078	Gaussian	0.068	FP	0.000
W	La	1	None	0.000	14.0273	Gaussian	0.000	FP	0.000
Pb	La	1	None	29.480	14.7092	Gaussian	0.023	FP	0.000

Analysis Report for Sand Sample B

	Thick	Type	Error	Units	Density	Norm.	Total
1	0.00	Bulk	0.00	mg/cm2	0.00F	On	100.00

Sample Table

Layer	Component	Type	Concn.	Error	Units	Mole%	Error
1	SiO2	Calc	75.924	1.711	wt.%	78.252	1.763
1	V2O5	Calc	0.031	0.015	wt.%	0.010	0.005
1	Cr2O3	Calc	0.093	0.011	wt.%	0.038	0.005
1	MnO	Calc	0.043	0.007	wt.%	0.038	0.006
1	Fe2O3	Calc	1.129	0.023	wt.%	0.438	0.009
1	CoO	Calc	0.029	0.008	wt.%	0.024	0.006
1	NiO	Calc	0.016	0.005	wt.%	0.013	0.004
1	CuO	Calc	0.045	0.005	wt.%	0.035	0.004
1	Nb2O5	Calc	0.012	0.007	wt.%	0.003	0.002
1	WO3	Calc	0.008	0.019	wt.%	0.002	0.005
1	P2O5	Calc	0.000	0.000	wt.%	0.000	0.000
1	SO3	Calc	0.353	0.137	wt.%	0.273	0.106
1	CaO	Calc	0.898	0.067	wt.%	0.991	0.074
1	MgO	Calc	0.000	0.000	wt.%	0.000	0.000
1	K2O	Calc	7.290	0.173	wt.%	4.793	0.114
1	BaO	Calc	0.144	0.078	wt.%	0.058	0.032
1	Al2O3	Calc	7.145	3.240	wt.%	4.340	1.968
1	Ta2O5	Calc	0.071	0.019	wt.%	0.010	0.003
1	TiO2	Calc	0.562	0.030	wt.%	0.436	0.024
1	ZnO	Calc	0.000	0.000	wt.%	0.000	0.000
1	Ag2O	Calc	0.023	0.041	wt.%	0.006	0.011
1	Cl	Calc	5.761	0.164	wt.%	10.063	0.286
1	ZrO2	Calc	0.055	0.007	wt.%	0.028	0.003
1	SnO2	Calc	0.264	0.520	wt.%	0.109	0.214
1	PbO	Calc	0.010	0.011	wt.%	0.003	0.003
1	Rb2O	Calc	0.026	0.004	wt.%	0.009	0.001
1	Cs2O	Calc	0.030	0.085	wt.%	0.007	0.019
1	SrO	Calc	0.036	0.005	wt.%	0.021	0.003

Element Table

International Journal of Engineering Research & Technology (IJERT)
ISSN: 2278-0181
Vol. 15 Issue 07 , July - 2026

Elmt	Line	Cond	Ratio	Intensity	Error	Intensity	Conc.	Conc
Calibration	Code	Code	Method	(c/s)	(c/s)	Method		
Method	Coefficient							
O	Ka	0	None	0.000	0.0000	Gaussian	46.255	None 0.000
Mg	Ka	1	None	0.000	3.9328	Gaussian	0.000	FP 0.000
Al	Ka	1	None	28.702	13.0152	Gaussian	3.782	FP 0.000
Si	Ka	1	None	1375.670	30.9939	Gaussian	35.491	FP 0.000
P	Ka	1	None	0.000	16.5741	Gaussian	0.000	FP 0.000
S	Ka	1	None	19.206	7.4644	Gaussian	0.142	FP 0.000
Cl	Ka	1	None	1017.357	28.8858	Gaussian	5.761	FP 0.000
K	Ka	1	None	1465.393	34.7601	Gaussian	6.052	FP 0.000
Ca	Ka	1	None	209.349	15.5379	Gaussian	0.642	FP 0.000
Ti	Ka	1	None	244.952	13.2130	Gaussian	0.337	FP 0.000
V	Ka	1	None	17.044	8.3092	Gaussian	0.017	FP 0.000
Cr	Ka	1	None	82.177	9.8942	Gaussian	0.064	FP 0.000
Mn	Ka	1	None	55.094	9.1878	Gaussian	0.034	FP 0.000
Fe	Ka	1	None	1578.954	32.2998	Gaussian	0.790	FP 0.000
Co	Ka	1	None	53.948	14.3711	Gaussian	0.023	FP 0.000
Ni	Ka	1	None	34.441	11.1032	Gaussian	0.013	FP 0.000
Cu	Ka	1	None	112.003	12.7402	Gaussian	0.036	FP 0.000
Zn	Ka	1	None	0.000	10.6767	Gaussian	0.000	FP 0.000
Rb	Ka	1	None	100.462	15.3333	Gaussian	0.024	FP 0.000
Sr	Ka	1	None	110.712	15.4774	Gaussian	0.030	FP 0.000
Zr	Ka	1	None	127.765	15.5872	Gaussian	0.041	FP 0.000
Nb	Ka	1	None	23.483	13.4358	Gaussian	0.008	FP 0.000
Ag	Ka	1	None	5.697	10.1871	Gaussian	0.021	FP 0.000
Sn	La	1	None	16.136	31.7647	Gaussian	0.208	FP 0.000
Cs	La	1	None	4.344	12.4801	Gaussian	0.028	FP 0.000
Ba	La	1	None	23.045	12.5996	Gaussian	0.129	FP 0.000
Ta	La	1	None	50.261	13.3052	Gaussian	0.058	FP 0.000
W	La	1	None	6.031	13.6590	Gaussian	0.007	FP 0.000
Pb	La	1	None	13.525	14.7337	Gaussian	0.009	FP 0.000

Tar	Filter	Thick.	kV	uA	Detector	Thick.	Atm	Preset
Actual	get	mg/cm2			Type	Filter	mg/cm2	
Time(s)	Time(s)							
1	Rh	None	0.00	30.0	60.0 SDD	None	0.00	Air 60.0 15.0

Analysis Report for Sand Sample C

	Thick	Type	Error	Units	Density	Norm.	Total
1	0.00	Bulk	0.00	mg/cm2	0.00F	On	100.00

Sample Table

Layer	Component	Type	Concn.	Error	Units	Mole%	Error
1	SiO2	Calc	78.531	1.753	wt.%	83.904	1.873
1	V2O5	Calc	0.056	0.014	wt.%	0.020	0.005
1	Cr2O3	Calc	0.071	0.010	wt.%	0.030	0.004
1	MnO	Calc	0.017	0.006	wt.%	0.015	0.005
1	Fe2O3	Calc	1.316	0.024	wt.%	0.529	0.009
1	CoO	Calc	0.006	0.007	wt.%	0.005	0.006
1	NiO	Calc	0.002	0.005	wt.%	0.002	0.004
1	CuO	Calc	0.071	0.005	wt.%	0.057	0.004
1	Nb2O5	Calc	0.010	0.006	wt.%	0.002	0.002
1	WO3	Calc	0.029	0.019	wt.%	0.008	0.005
1	P2O5	Calc	0.083	0.549	wt.%	0.038	0.248
1	SO3	Calc	0.326	0.113	wt.%	0.261	0.091
1	CaO	Calc	1.437	0.072	wt.%	1.645	0.083

International Journal of Engineering Research & Technology (IJERT)
ISSN: 2278-0181
Vol. 15 Issue 07 , July - 2026

1	MgO	Calc	0.000	0.000	wt.%	0.000	0.000
1	K2O	Calc	6.136	0.152	wt.%	4.182	0.103
1	BaO	Calc	0.199	0.070	wt.%	0.083	0.029
1	Al2O3	Calc	9.083	3.269	wt.%	5.719	2.058
1	Ta2O5	Calc	0.084	0.020	wt.%	0.012	0.003
1	TiO2	Calc	0.482	0.027	wt.%	0.387	0.021
1	ZnO	Calc	0.000	0.000	wt.%	0.000	0.000
1	Ag2O	Calc	0.003	0.040	wt.%	0.001	0.011
1	Cl	Calc	1.607	0.089	wt.%	2.909	0.160
1	ZrO2	Calc	0.063	0.006	wt.%	0.033	0.003
1	SnO2	Calc	0.247	0.471	wt.%	0.105	0.200
1	PbO	Calc	0.028	0.010	wt.%	0.008	0.003
1	Rb2O	Calc	0.032	0.004	wt.%	0.011	0.001
1	Cs2O	Calc	0.049	0.079	wt.%	0.011	0.018
1	SrO	Calc	0.032	0.005	wt.%	0.020	0.003

Element Table	Elmt	Line	Cond	Ratio	Intensity	Error	Intensity	Conc.	Conc	Calibration
Code	Code					Method	(c/s)	(c/s)	Method	Method
Coefficient										
O	Ka	0	None	0.000	0.0000	Gaussian	48.574	None	0.000	
Mg	Ka	1	None	0.000	4.0310	Gaussian	0.000	FP	0.000	
Al	Ka	1	None	37.165	13.3769	Gaussian	4.807	FP	0.000	
Si	Ka	1	None	1413.531	31.5561	Gaussian	36.709	FP	0.000	
P	Ka	1	None	2.513	16.5557	Gaussian	0.036	FP	0.000	
S	Ka	1	None	17.608	6.1074	Gaussian	0.130	FP	0.000	
Cl	Ka	1	None	288.580	15.9034	Gaussian	1.607	FP	0.000	
K	Ka	1	None	1359.352	33.5937	Gaussian	5.094	FP	0.000	
Ca	Ka	1	None	373.639	18.7790	Gaussian	1.027	FP	0.000	
Ti	Ka	1	None	231.491	12.8072	Gaussian	0.289	FP	0.000	
V	Ka	1	None	34.564	8.7356	Gaussian	0.032	FP	0.000	
Cr	Ka	1	None	69.144	9.6509	Gaussian	0.049	FP	0.000	
Mn	Ka	1	None	23.785	8.2997	Gaussian	0.013	FP	0.000	
Fe	Ka	1	None	2024.789	36.3342	Gaussian	0.920	FP	0.000	
Co	Ka	1	None	13.292	15.2300	Gaussian	0.005	FP	0.000	
Ni	Ka	1	None	5.423	10.6578	Gaussian	0.002	FP	0.000	
Cu	Ka	1	None	194.328	14.5284	Gaussian	0.056	FP	0.000	
Zn	Ka	1	None	0.000	11.4029	Gaussian	0.000	FP	0.000	
Rb	Ka	1	None	131.676	15.9572	Gaussian	0.029	FP	0.000	
Sr	Ka	1	None	107.647	15.4855	Gaussian	0.027	FP	0.000	
Zr	Ka	1	None	157.870	16.2120	Gaussian	0.046	FP	0.000	
Nb	Ka	1	None	21.732	13.6131	Gaussian	0.007	FP	0.000	
Ag	Ka	1	None	0.748	10.8642	Gaussian	0.003	FP	0.000	
Sn	La	1	None	16.580	31.6055	Gaussian	0.194	FP	0.000	
Cs	La	1	None	7.852	12.7776	Gaussian	0.046	FP	0.000	
Ba	La	1	None	35.240	12.3696	Gaussian	0.178	FP	0.000	
Ta	La	1	None	64.887	15.1668	Gaussian	0.068	FP	0.000	
W	La	1	None	23.126	15.4580	Gaussian	0.023	FP	0.000	
Pb	La	1	None	41.343	14.9786	Gaussian	0.026	FP	0.000	

Tar	Filter	Thick.	kV	uA	Detector	Thick.	Atm	Preset	Actual	get
		mg/cm2			Type	Filter	mg/cm2		Time(s)	Time(s)
1	Rh	None	0.00	30.0	60.0	SDD	None	0.00	Air	60.0	15.0

Analysis Report for Sand Sample D

Thick	Type	Error	Units	Density	Norm.	Total
1 0.00	Bulk	0.00	mg/cm2	0.00F	On	100.00

International Journal of Engineering Research & Technology (IJERT)
ISSN: 2278-0181
Vol. 15 Issue 07 , July - 2026

Sample Table

Layer	Component	Type	Concn.	Error	Units	Mole%	Error
1	SiO2	Calc	78.512	1.710	wt.%	83.187	1.812
1	V2O5	Calc	0.000	0.000	wt.%	0.000	0.000
1	Cr2O3	Calc	0.027	0.008	wt.%	0.011	0.004
1	MnO	Calc	0.017	0.006	wt.%	0.015	0.005
1	Fe2O3	Calc	1.086	0.021	wt.%	0.433	0.008
1	CoO	Calc	0.007	0.007	wt.%	0.006	0.006
1	NiO	Calc	0.002	0.004	wt.%	0.002	0.003
1	CuO	Calc	0.042	0.004	wt.%	0.034	0.004
1	Nb2O5	Calc	0.008	0.006	wt.%	0.002	0.001
1	WO3	Calc	0.006	0.017	wt.%	0.002	0.005
1	P2O5	Calc	0.059	0.527	wt.%	0.027	0.236
1	SO3	Calc	0.483	0.120	wt.%	0.384	0.095
1	CaO	Calc	1.447	0.072	wt.%	1.643	0.081
1	MgO	Calc	0.000	0.000	wt.%	0.000	0.000
1	K2O	Calc	6.468	0.153	wt.%	4.371	0.103
1	BaO	Calc	0.126	0.045	wt.%	0.052	0.018
1	Al2O3	Calc	8.950	3.169	wt.%	5.588	1.979
1	Ta2O5	Calc	0.032	0.016	wt.%	0.005	0.002
1	TiO2	Calc	0.160	0.017	wt.%	0.127	0.014
1	ZnO	Calc	0.006	0.004	wt.%	0.005	0.003
1	Ag2O	Calc	0.024	0.039	wt.%	0.007	0.011
1	Cl	Calc	2.202	0.100	wt.%	3.954	0.179
1	ZrO2	Calc	0.027	0.005	wt.%	0.014	0.003
1	SnO2	Calc	0.227	0.471	wt.%	0.096	0.199
1	PbO	Calc	0.019	0.009	wt.%	0.005	0.003
1	Rb2O	Calc	0.027	0.004	wt.%	0.009	0.001
1	Cs2O	Calc	0.002	0.056	wt.%	0.000	0.013
1	SrO	Calc	0.031	0.004	wt.%	0.019	0.003

Element Table

Elmt	Line	Cond	Ratio	Intensity	Error	Intensity	Conc.	Conc
	Calibration	Code	Code	Method	(c/s)	(c/s)	Method	
	Method	Coefficient						
O	Ka	0	None	0.000		0.0000	Gaussian	48.362 None 0.000
Mg	Ka	1	None	0.000		4.1269	Gaussian	0.000 FP 0.000
Al	Ka	1	None	38.706		13.7046	Gaussian	4.737 FP 0.000
Si	Ka	1	None	1495.451		32.5742	Gaussian	36.700 FP 0.000
P	Ka	1	None	1.888		16.7142	Gaussian	0.026 FP 0.000
S	Ka	1	None	27.497		6.8332	Gaussian	0.193 FP 0.000
Cl	Ka	1	None	415.293		18.8436	Gaussian	2.202 FP 0.000
K	Ka	1	None	1486.324		35.0433	Gaussian	5.370 FP 0.000
Ca	Ka	1	None	388.106		19.2109	Gaussian	1.034 FP 0.000
Ti	Ka	1	None	79.365		8.5359	Gaussian	0.096 FP 0.000
V	Ka	1	None	0.000		7.7860	Gaussian	0.000 FP 0.000
Cr	Ka	1	None	27.479		8.6268	Gaussian	0.019 FP 0.000
Mn	Ka	1	None	24.990		8.8351	Gaussian	0.013 FP 0.000
Fe	Ka	1	None	1759.166		34.0586	Gaussian	0.759 FP 0.000
Co	Ka	1	None	15.439		14.4994	Gaussian	0.006 FP 0.000
Ni	Ka	1	None	5.295		10.1469	Gaussian	0.002 FP 0.000
Cu	Ka	1	None	123.773		12.9646	Gaussian	0.034 FP 0.000
Zn	Ka	1	None	21.127		11.6489	Gaussian	0.005 FP 0.000

International Journal of Engineering Research & Technology (IJERT)
ISSN: 2278-0181
Vol. 15 Issue 07 , July - 2026

Rb	Ka	1	None	118.877	15.7250	Gaussian	0.024 FP	0.000
Sr	Ka	1	None	113.735	15.5538	Gaussian	0.026 FP	0.000
Zr	Ka	1	None	73.740	14.7091	Gaussian	0.020 FP	0.000
Nb	Ka	1	None	18.442	13.5926	Gaussian	0.006 FP	0.000
Ag	Ka	1	None	6.986	11.5029	Gaussian	0.022 FP	0.000
Sn	La	1	None	15.840	32.8351	Gaussian	0.179 FP	0.000
Cs	La	1	None	0.286	9.2897	Gaussian	0.002 FP	0.000
Ba	La	1	None	23.102	8.1568	Gaussian	0.113 FP	0.000
Ta	La	1	None	26.620	13.5077	Gaussian	0.026 FP	0.000
W	La	1	None	4.958	14.0490	Gaussian	0.005 FP	0.000
Pb	La	1	None	29.463	14.6241	Gaussian	0.017 FP	0.000

Analysis Conditions

Tar	Filter	Thick.	kV	uA	---Detector---		Thick.	Atm	
Preset	Actual	get			mg/cm2	Type	Filter		
mg/cm2	Time(s)	Time(s)							
1	Rh	None	0.00	30.0	60.0	SDD	None	0.00	Air 60.0 15.0

Analysis Report for Sand Sample E

	Thick	Type	Error	Units	Density	Norm.	Total
1	0.00	Bulk	0.00	mg/cm2	0.00F	On	100.00

Sample Table

Layer	Component	Type	Concn.	Error	Units	Mole%	Error
1	SiO2	Calc	76.438	1.735	wt.%	79.788	1.811
1	V2O5	Calc	0.000	0.000	wt.%	0.000	0.000
1	Cr2O3	Calc	0.041	0.009	wt.%	0.017	0.004
1	MnO	Calc	0.026	0.007	wt.%	0.023	0.006
1	Fe2O3	Calc	1.295	0.024	wt.%	0.509	0.010
1	CoO	Calc	0.026	0.008	wt.%	0.022	0.006
1	NiO	Calc	0.015	0.005	wt.%	0.012	0.004
1	CuO	Calc	0.060	0.005	wt.%	0.048	0.004
1	Nb2O5	Calc	0.009	0.007	wt.%	0.002	0.002
1	WO3	Calc	0.005	0.018	wt.%	0.001	0.005
1	P2O5	Calc	0.101	0.543	wt.%	0.045	0.240
1	SO3	Calc	0.602	0.144	wt.%	0.472	0.112
1	CaO	Calc	1.981	0.086	wt.%	2.215	0.096
1	MgO	Calc	0.000	0.000	wt.%	0.000	0.000
1	K2O	Calc	6.499	0.162	wt.%	4.327	0.108
1	BaO	Calc	0.144	0.056	wt.%	0.059	0.023
1	Al2O3	Calc	7.776	3.265	wt.%	4.783	2.008
1	Ta2O5	Calc	0.069	0.019	wt.%	0.010	0.003
1	TiO2	Calc	0.258	0.021	wt.%	0.203	0.017
1	ZnO	Calc	0.005	0.004	wt.%	0.004	0.003
1	Ag2O	Calc	0.021	0.043	wt.%	0.006	0.012
1	Cl	Calc	4.084	0.139	wt.%	7.225	0.246
1	ZrO2	Calc	0.025	0.006	wt.%	0.013	0.003
1	SnO2	Calc	0.454	0.512	wt.%	0.189	0.213
1	PbO	Calc	0.016	0.011	wt.%	0.005	0.003
1	Rb2O	Calc	0.026	0.004	wt.%	0.009	0.001
1	Cs2O	Calc	0.000	0.000	wt.%	0.000	0.000
1	SrO	Calc	0.024	0.005	wt.%	0.014	0.003

Element Table

International Journal of Engineering Research & Technology (IJERT)
ISSN: 2278-0181
Vol. 15 Issue 07 , July - 2026

Elmt	Line	Cond	Ratio	Intensity	Error	Intensity	Conc.	Conc
Calibration	Code	Code	Method	(c/s)	(c/s)	Method		
Method	Coefficient							
O	Ka	0	None	0.000	0.0000	Gaussian	47.130	None 0.000
Mg	Ka	1	None	0.000	3.9508	Gaussian	0.000	FP 0.000
Al	Ka	1	None	31.086	13.0533	Gaussian	4.115	FP 0.000
Si	Ka	1	None	1368.917	31.0732	Gaussian	35.731	FP 0.000
P	Ka	1	None	3.035	16.3623	Gaussian	0.044	FP 0.000
S	Ka	1	None	32.480	7.7462	Gaussian	0.241	FP 0.000
Cl	Ka	1	None	721.094	24.5320	Gaussian	4.084	FP 0.000
K	Ka	1	None	1348.048	33.5584	Gaussian	5.395	FP 0.000
Ca	Ka	1	None	480.165	20.7951	Gaussian	1.416	FP 0.000
Ti	Ka	1	None	114.361	9.4877	Gaussian	0.155	FP 0.000
V	Ka	1	None	0.000	7.6245	Gaussian	0.000	FP 0.000
Cr	Ka	1	None	36.868	8.4801	Gaussian	0.028	FP 0.000
Mn	Ka	1	None	34.237	8.6241	Gaussian	0.020	FP 0.000
Fe	Ka	1	None	1853.446	34.7956	Gaussian	0.906	FP 0.000
Co	Ka	1	None	50.052	14.6829	Gaussian	0.020	FP 0.000
Ni	Ka	1	None	31.515	10.4993	Gaussian	0.011	FP 0.000
Cu	Ka	1	None	154.309	13.0030	Gaussian	0.048	FP 0.000
Zn	Ka	1	None	13.935	10.3666	Gaussian	0.004	FP 0.000
Rb	Ka	1	None	99.294	15.4030	Gaussian	0.023	FP 0.000
Sr	Ka	1	None	74.562	14.9229	Gaussian	0.020	FP 0.000
Zr	Ka	1	None	58.817	14.7152	Gaussian	0.018	FP 0.000
Nb	Ka	1	None	18.515	13.4962	Gaussian	0.007	FP 0.000
Ag	Ka	1	None	5.280	10.8347	Gaussian	0.019	FP 0.000
Sn	La	1	None	28.526	32.1601	Gaussian	0.358	FP 0.000
Cs	La	1	None	0.000	10.2085	Gaussian	0.000	FP 0.000
Ba	La	1	None	23.401	9.0598	Gaussian	0.129	FP 0.000
Ta	La	1	None	49.611	13.3760	Gaussian	0.056	FP 0.000
W	La	1	None	4.024	13.7213	Gaussian	0.004	FP 0.000
Pb	La	1	None	22.156	14.4471	Gaussian	0.015	FP 0.000

Analysis Conditions

Tar	Filter	Thick.	kV	uA	---Detector---		Thick.	Atm
Preset	Actual	get			mg/cm2	Type	Filter	
mg/cm2	Time(s)	Time(s)						

3.2.1 Silicon Dioxide (SiO_2)

Silicon dioxide is the primary constituent of all the samples, with the following concentrations:

Sample	SiO_2 (wt.%)
A	79.60
B	75.92
C	78.53
D	78.51
E	76.44

The SiO_2 content ranges from **75.92% to 79.60%**, with **Sample A** having the highest silica concentration. This demonstrates that Wudil River sand is naturally rich in silica and therefore represents a promising source for silica production. Nevertheless, the silica content is lower than the **98–99.5% SiO_2** generally required for high-purity industrial silica used in advanced polymer composites and photovoltaic applications. Consequently, the raw sand cannot be used directly and must undergo purification to remove mineral impurities.

3.2.2 Iron Oxide (Fe_2O_3)

International Journal of Engineering Research & Technology (IJERT)
ISSN: 2278-0181
Vol. 15 Issue 07 , July - 2026

Iron oxide concentrations are:

- Sample A – 1.405%
- Sample B – 1.129%
- Sample C – 1.316%
- Sample D – 1.086%
- Sample E – 1.295%

Iron oxide is one of the most significant impurities in silica sand because it reduces the whiteness of the silica and adversely affects optical and thermal properties. For silica intended for PVC solar panel components, iron should ideally be below 0.05–0.10**%** after purification. Although the measured Fe_2O_3 contents are relatively low for natural river sand, they remain too high for direct industrial application. Acid leaching using hydrochloric acid (HCl), sulfuric acid (H_2SO_4), or oxalic acid would be expected to substantially reduce the iron content. Among the samples, Sample D contains the lowest Fe_2O_3 concentration (1.086%), making it the most favorable with respect to iron impurity.

3.2.3 Aluminium Oxide (Al_2O_3)

The aluminium oxide concentrations are:

- Sample A – 6.81%
- Sample B – 7.15%
- Sample C – 9.08%
- Sample D – 8.95%
- Sample E – 7.78%

The relatively high Al_2O_3 content suggests the presence of feldspar and clay minerals. These minerals reduce silica purity and should be removed through washing, classification, and acid treatment before silica extraction. Samples A and B contain slightly lower alumina levels and would therefore require comparatively less purification.

3.2.4 Potassium Oxide (K_2O)

Potassium oxide concentrations range from 6.14% to 7.29%, indicating the presence of potassium-bearing feldspar minerals.

Although K_2O does not prevent silica extraction, it lowers silica purity and must be removed during beneficiation. The high K_2O levels suggest that the Wudil River sand contains appreciable feldspathic material, which can be reduced by flotation or magnetic separation combined with chemical leaching.

3.2.5 Calcium Oxide (CaO)

Calcium oxide concentrations vary between 0.90% and 1.98%.

These values indicate the presence of carbonate or calcareous minerals. Since calcium compounds can interfere with high-purity silica production, they should be removed during acid washing. Sample B has the lowest CaO content, whereas Sample E has the highest.

3.2.6 Titanium Oxide (TiO_2)

TiO_2 concentrations range from 0.16% to 1.23%.

Titanium-bearing minerals contribute to discoloration and reduce silica quality. These minerals can usually be reduced by gravity separation, magnetic separation, or acid leaching. Sample D contains the lowest TiO_2 concentration, indicating better natural purity.

3.2.7 Chlorine (Cl)

The chlorine contents range from 1.27% to 5.76**%**, with Sample B exhibiting the highest value. Elevated chlorine levels may result from soluble salts deposited during river transport. These salts

International Journal of Engineering Research & Technology (IJERT)
ISSN: 2278-0181
Vol. 15 Issue 07 , July - 2026

should be effectively removed by repeated washing before silica purification to prevent contamination during processing.

3.2.8 Trace Elements

Trace oxides such as Cr_2O_3, MnO, CuO, NiO, CoO, ZnO, ZrO_2, Nb_2O_5, PbO, and BaO are present only in very small quantities (generally below 0.3 wt.%). These concentrations are unlikely to significantly affect silica extraction but would be further reduced during beneficiation and purification.

3.2.8 Suitability for Silica Extraction

The XRF results demonstrate that Wudil River sand possesses good potential as a silica source because:

- SiO_2 is the dominant oxide (approximately 76–80 wt.%).
- Iron oxide is relatively low compared with many natural sands.
- Most impurities occur at moderate or trace concentrations.
- The chemical composition is suitable for beneficiation to produce higher-purity silica.

However, the raw sand does not yet meet the purity requirements for PVC solar panel manufacturing. The silica content must be increased to above 98%, while iron, aluminium, alkali oxides, calcium, and titanium must be significantly reduced through appropriate processing.

For PVC solar panel production, purified silica is commonly incorporated as a reinforcing filler to improve:

- mechanical strength,
- dimensional stability,
- thermal resistance,
- UV resistance, and
- durability of the PVC composite.

The XRF results indicate that Wudil River sand is a promising raw material for this purpose after purification. Samples with higher SiO_2 and lower impurity levels would require less beneficiation and lower processing costs.

Considering both silica content and impurity levels:

- **Sample A** has the highest SiO_2 content (79.60 wt.%) and is the best candidate from the standpoint of silica abundance.
- **Sample D** has slightly lower SiO_2 (78.51 wt.%) but the lowest Fe_2O_3 (1.086 wt.%) and the lowest TiO_2 (0.16 wt.%), making it particularly attractive because iron and titanium are among the most problematic impurities.
- **Samples C and B** are also suitable but would require somewhat greater impurity removal.
- **Sample E** is the least favorable due to its lower SiO_2 content and comparatively higher CaO and Cl contents.

3.3 Scanning Electron Microscopy (SEM) analysis

The Scanning Electron Microscopy (SEM) analysis of the Wudil River sand samples was carried out at magnifications of **250×, 500×, and 800×** using a Backscattered Electron (BSE) detector operating

International Journal of Engineering Research & Technology (IJERT)
ISSN: 2278-0181
Vol. 15 Issue 07 , July - 2026

at **5 kV**. The SEM micrographs provide valuable information on the particle morphology, grain shape, surface texture, particle size, and distribution of impurities, all of which influence the efficiency of silica extraction and the suitability of the extracted silica as a reinforcing filler in PVC solar panel materials.

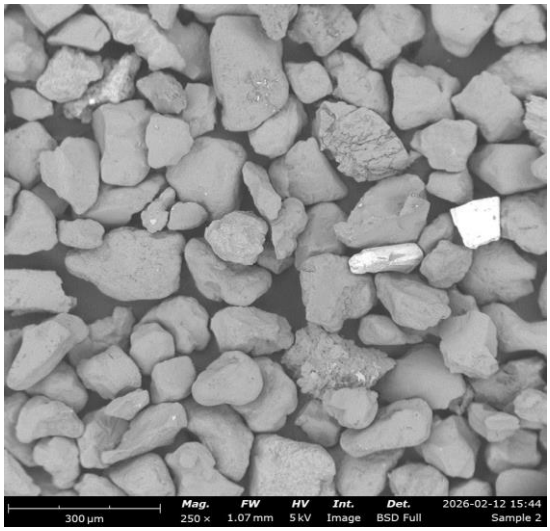

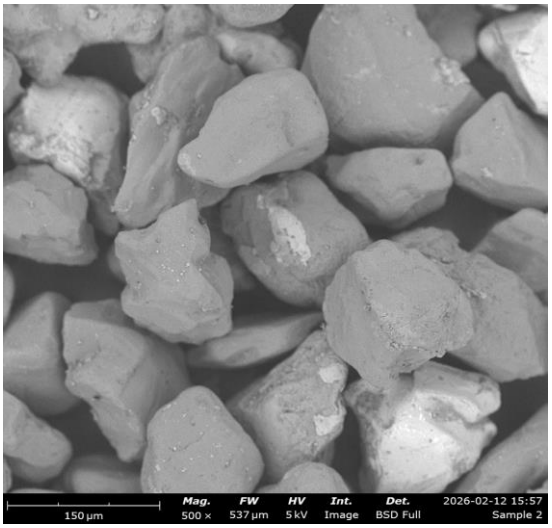

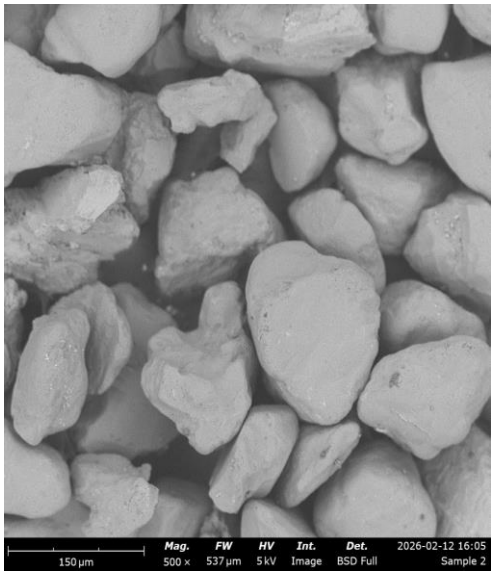

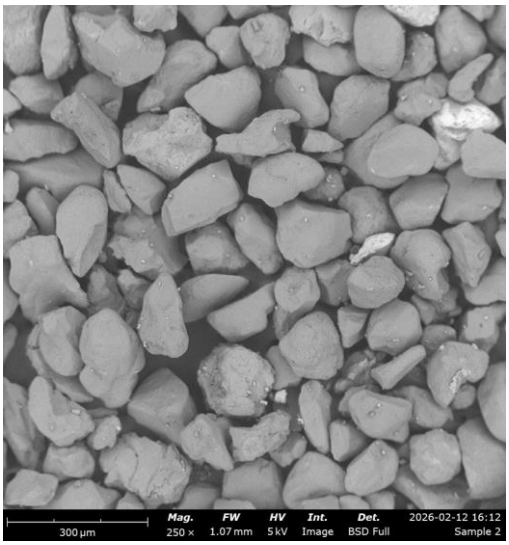

International Journal of Engineering Research & Technology (IJERT)
ISSN: 2278-0181
Vol. 15 Issue 07 , July - 2026

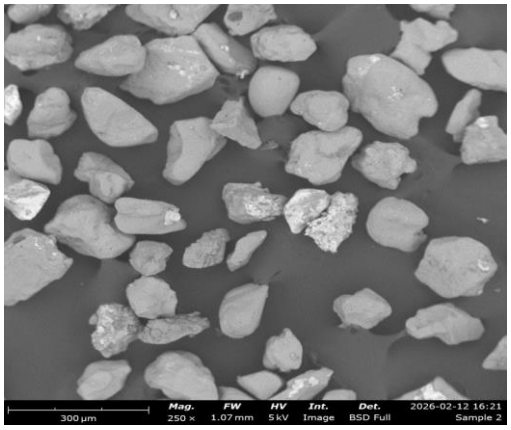

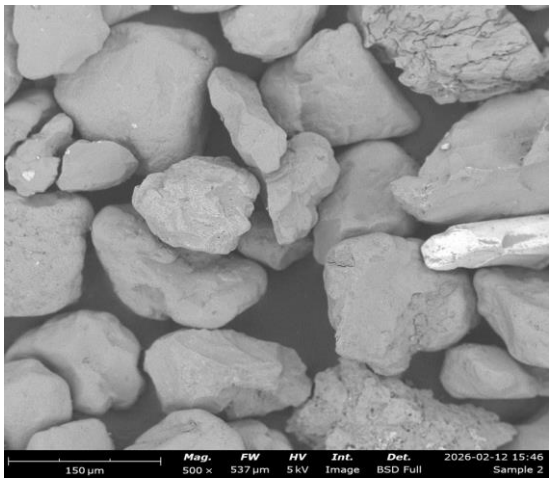

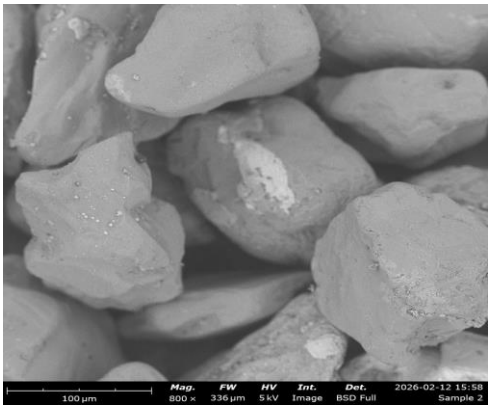

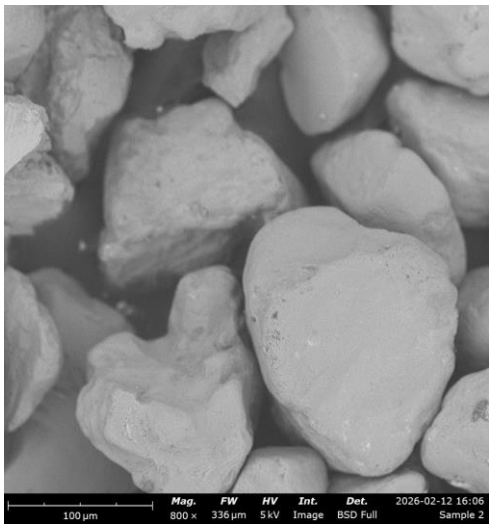

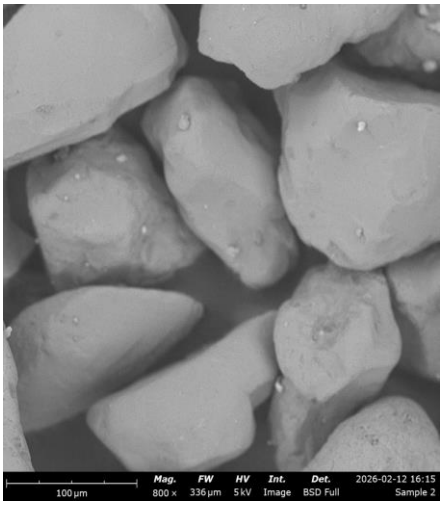

International Journal of Engineering Research & Technology (IJERT)
ISSN: 2278-0181
Vol. 15 Issue 07 , July - 2026

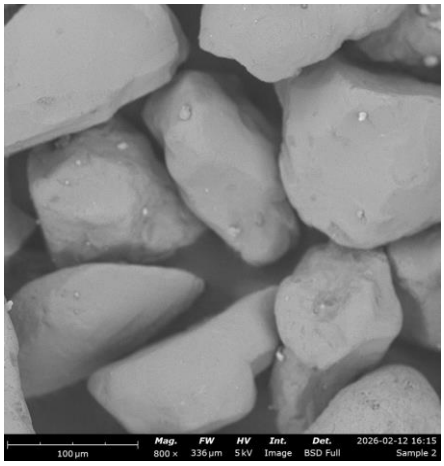

3.3.1 Particle Shape and Morphology

The SEM micrographs reveal that the Wudil River sand consists predominantly of sub-angular to sub-rounded grains, with a few angular particles observed throughout the samples. The majority of the grains exhibit irregular polygonal shapes with rounded edges, indicating that the particles have undergone moderate weathering and fluvial transport within the river system before deposition.

Quartz grains generally retain their crystalline geometry despite partial abrasion during transportation. The observed sub-angular morphology is characteristic of river-derived silica sand and suggests that the grains have experienced sufficient mechanical erosion to remove sharp edges while maintaining the structural integrity of the quartz crystals.

This particle morphology is advantageous during silica extraction because sub-angular grains possess a relatively large specific surface area, allowing acid solutions to readily penetrate and dissolve surface impurities such as iron oxides, aluminosilicates, and carbonate minerals.

3.3.2 Surface Texture

At 500× and 800× magnifications, most quartz particles exhibit relatively smooth and compact surfaces, although localized rough regions, shallow pits, scratches, and fractured edges are evident on several grains. The smooth surfaces indicate that many particles consist of well-crystallized quartz with minimal weathering. Conversely, the roughened areas are likely associated with:

- adhered clay minerals,
- iron oxide coatings,
- feldspathic impurities,
- weathered mineral inclusions, or
- fractured quartz surfaces produced during sediment transport.

These rough surfaces are particularly important because they provide additional reaction sites during acid leaching. Hydrochloric acid or sulfuric acid can penetrate these irregularities more effectively, facilitating the dissolution of impurity minerals while leaving the chemically resistant quartz largely unaffected.

3.3.3 Grain Size Distribution

The SEM images show particles ranging approximately from 100 µm to 500 µm, which agrees well with the sieve analysis where most particles were retained between the 300 µm and 600 µm sieve fractions.

International Journal of Engineering Research & Technology (IJERT)
ISSN: 2278-0181
Vol. 15 Issue 07 , July - 2026

The relatively uniform particle size distribution indicates effective natural sorting by river action. Uniform particle sizes are desirable during silica beneficiation because they:

- improve washing efficiency,
- enhance magnetic separation,
- permit uniform acid penetration,
- reduce processing time, and
- improve silica recovery.

The agreement between SEM observations and the sieve analysis confirms that the Wudil River sand possesses a consistent particle size suitable for industrial beneficiation.

3.3.4 Surface Defects and Fractures

Several particles exhibit:

- fractured edges,
- micro-cracks,
- shallow depressions,
- chipped corners, and
- cleavage-like features.

These structural defects are beneficial for silica purification because they increase the exposed surface area available for chemical reactions during acid leaching.

The micro-cracks provide pathways through which acids can dissolve impurities trapped within the outer layers of the particles without significantly attacking the quartz itself.

Consequently, the morphology observed by SEM suggests that high silica recovery can be achieved using conventional beneficiation processes.

3.3.5 Presence of Surface Impurities

Although most particles appear relatively clean, several grains exhibit rough coatings and bright patches in the BSE images. These brighter regions are likely associated with minerals having higher average atomic numbers than quartz, including:

- iron oxides,
- titanium-bearing minerals,
- feldspars,
- aluminosilicates, or
- other heavy mineral impurities.

This observation agrees closely with the XRF analysis, which detected measurable quantities of:

- Fe_2O_3,
- Al_2O_3,
- TiO_2,
- CaO,
- K_2O, and
- trace metallic oxides.

The occurrence of these impurities primarily on grain surfaces suggests that they can be effectively removed by:

- washing,
- attrition scrubbing,
- magnetic separation, and
- acid leaching.

Therefore, the SEM results indicate that most impurities occur as surface coatings rather than being uniformly distributed within the quartz grains, making purification considerably easier.

3.3.6 Particle Packing and Dispersion

The lower magnification (250×) micrographs demonstrate that the particles are well dispersed with limited agglomeration. Individual grains remain largely separated from one another, indicating that the sand contains little cementing material.

International Journal of Engineering Research & Technology (IJERT)
ISSN: 2278-0181
Vol. 15 Issue 07 , July - 2026

The absence of severe particle agglomeration is advantageous because:

- washing becomes more effective,
- acids have unrestricted access to particle surfaces,
- beneficiation efficiency increases,
- silica recovery improves.

3.3.7 Quartz Grain Integrity

Most particles retain compact interiors without evidence of extensive internal porosity.
Quartz is naturally resistant to chemical weathering, and the SEM images demonstrate that the grains possess good structural integrity despite minor surface abrasion. The high mechanical stability of the quartz grains supports their use as a raw material for producing high-purity silica suitable for industrial applications.

3.3.8 Correlation with XRF Results

The SEM observations correlate well with the XRF chemical analysis. The XRF results indicated that the Wudil River sand contains approximately 76–80 wt.% SiO_2, confirming quartz as the dominant mineral phase. The smooth quartz-rich particles observed in the SEM micrographs support this finding. Likewise, the rough surface coatings and brighter mineral patches visible on some grains correspond to the presence of Fe_2O_3, Al_2O_3, TiO_2, K_2O, and CaO detected by XRF. Because these impurities are mainly concentrated on the grain surfaces, they are expected to be removed efficiently during beneficiation, thereby increasing the silica purity to levels suitable for industrial use.

3.3.8 Implications for Silica Extraction

The SEM morphology indicates that the Wudil River sand possesses several favourable characteristics for silica extraction:

- quartz grains dominate the sample;
- particles are mostly sub-angular to sub-rounded;
- surfaces are largely clean with only localized impurity coatings;
- fractures and micro-cracks facilitate acid penetration;
- particle sizes are relatively uniform;
- little agglomeration is observed.

These characteristics suggest that beneficiation through washing, sieving, magnetic separation, and acid leaching should substantially increase the silica content while reducing iron, alumina, titanium, and alkali impurities.

3.3.9 Relevance to PVC Solar Panel Manufacturing

Silica extracted from Wudil River sand can be incorporated into PVC composites as a reinforcing mineral filler. The morphology observed by SEM indicates that the purified silica would possess characteristics favourable for composite manufacturing. The irregular yet relatively smooth particles are expected to disperse effectively within the PVC matrix after milling, promoting good filler–polymer interfacial adhesion. Well-dispersed silica particles enhance the composite by:

- increasing tensile and flexural strength,
- improving hardness and abrasion resistance,
- enhancing thermal stability,
- improving dimensional stability,
- increasing ultraviolet (UV) resistance,
- reducing thermal expansion, and
- extending the service life of PVC solar panel components exposed to outdoor conditions.

Furthermore, the limited amount of surface contamination observed suggests that, after purification, the silica would exhibit improved compatibility with polymer matrices and contribute to higher-performance PVC composites.

3.4 Energy Dispersive X-ray Spectroscopy (EDX)

Energy Dispersive X-ray Spectroscopy (EDX) was employed alongside Scanning Electron Microscopy (SEM) to determine the elemental composition of the Wudil River sand samples (A–E). The EDX analysis provides localized elemental information from selected regions of the sand grains and

International Journal of Engineering Research & Technology (IJERT)
ISSN: 2278-0181
Vol. 15 Issue 07 , July - 2026

complements the XRF results by identifying the elements present on the particle surfaces. According to the EDX report, all five samples were analysed under identical operating conditions (5 kV accelerating voltage, BSD detector, and field of view of 671 μm). Notably, the report indicates that oxygen (O) and boron (B) were disabled during the analysis, meaning oxygen was not included in the quantitative results.

International Journal of Engineering Research & Technology (IJERT)
ISSN: 2278-0181
Vol. 15 Issue 07 , July - 2026

A EDX

1. region

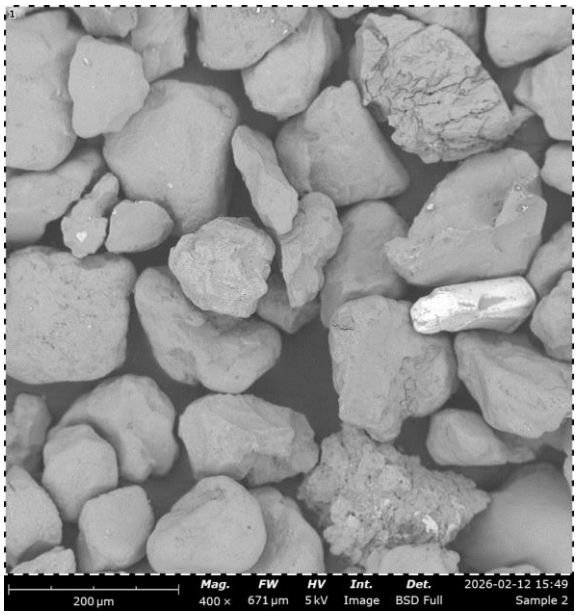

Element Number	Element Symbol	Element Name	Atomic Conc.	Weight Conc.
24	Cr	Chromium	95.99	93.42
38	Sr	Strontium	4.01	6.58

FOV: 671 µm, Mode: 5kV - Image, Detector: BSD Full, Time: FEB 12 2026 15:49

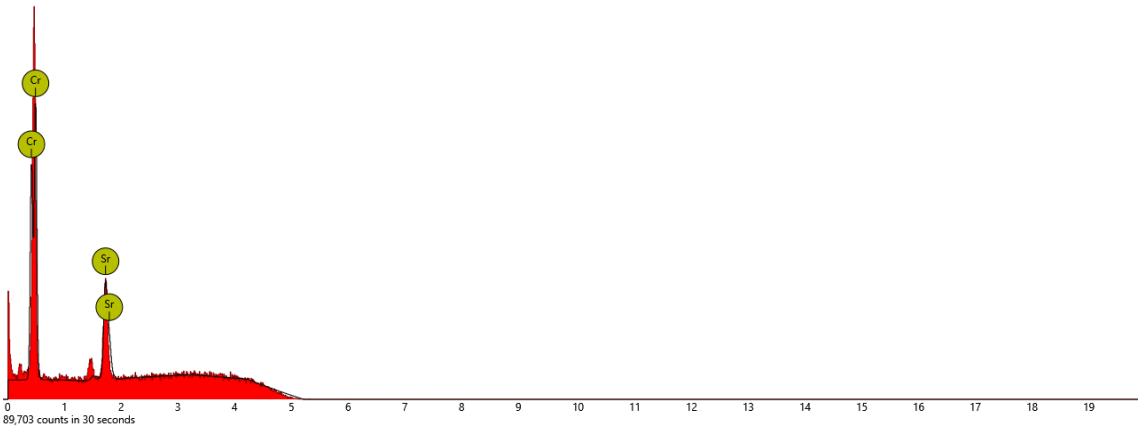

Disabled elements: B, O

International Journal of Engineering Research & Technology (IJERT)
ISSN: 2278-0181
Vol. 15 Issue 07 , July - 2026

B EDX

1. region

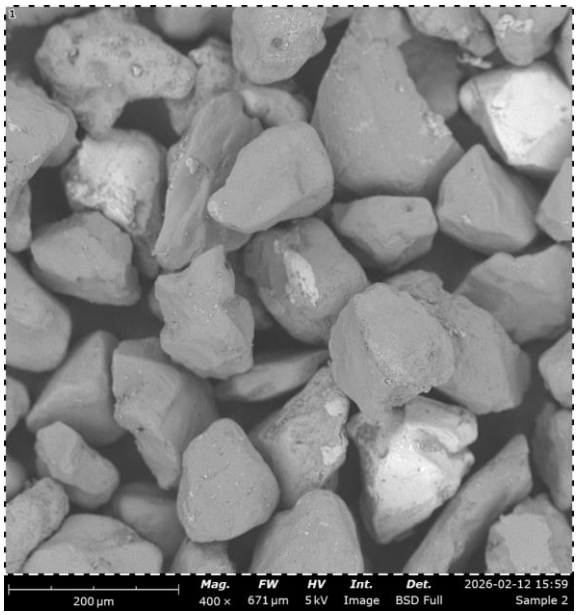

Element Number	Element Symbol	Element Name	Atomic Conc.	Weight Conc.
24	Cr	Chromium	95.92	93.31
38	Sr	Strontium	4.08	6.69

FOV: 671 µm, Mode: 5kV - Image, Detector: BSD Full, Time: FEB 12 2026 15:59

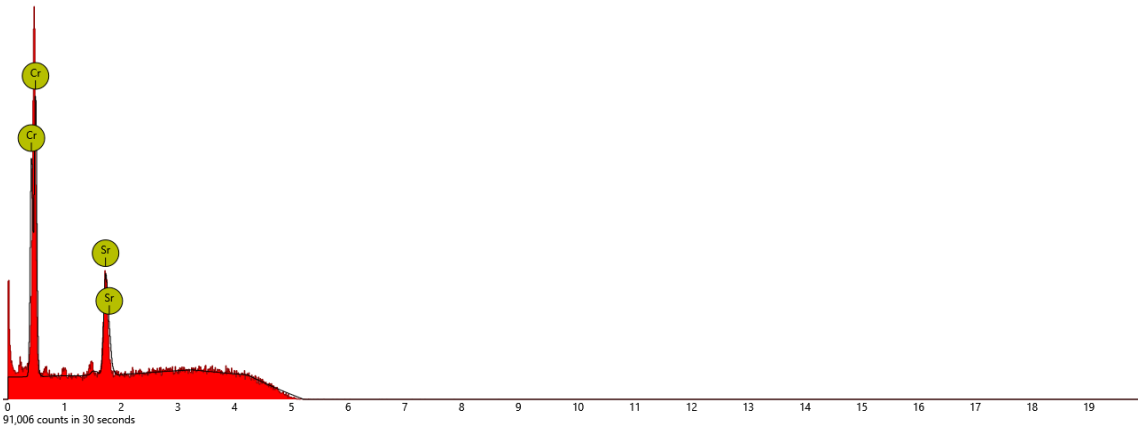

Disabled elements: B, O

International Journal of Engineering Research & Technology (IJERT)
ISSN: 2278-0181
Vol. 15 Issue 07 , July - 2026

C EDX

1. region

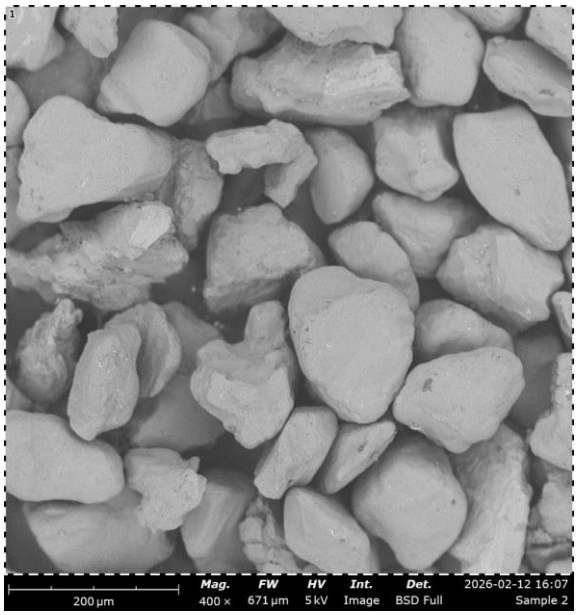

Element Number	Element Symbol	Element Name	Atomic Conc.	Weight Conc.
24	Cr	Chromium	95.56	92.73
38	Sr	Strontium	4.44	7.27

FOV: 671 µm, Mode: 5kV - Image, Detector: BSD Full, Time: FEB 12 2026 16:07

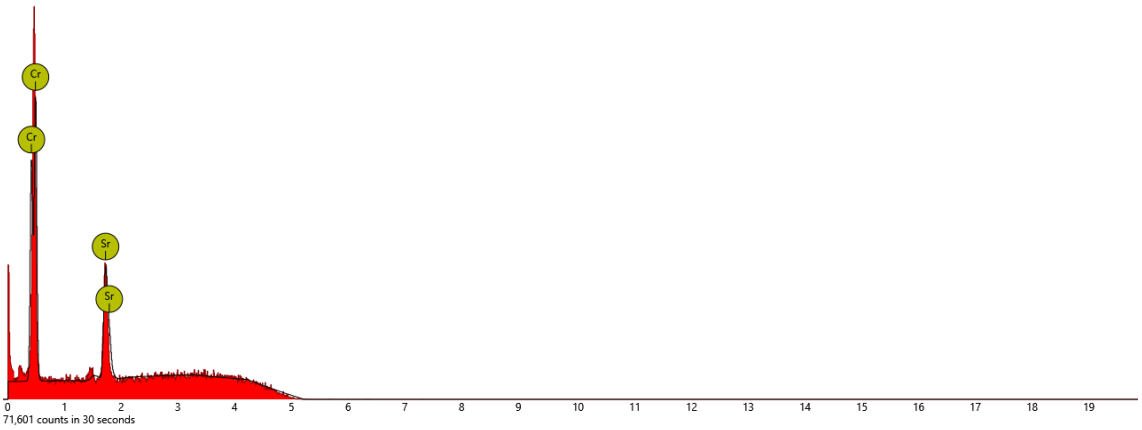

Disabled elements: B, O

International Journal of Engineering Research & Technology (IJERT)
ISSN: 2278-0181
Vol. 15 Issue 07 , July - 2026

D EDX

1. region

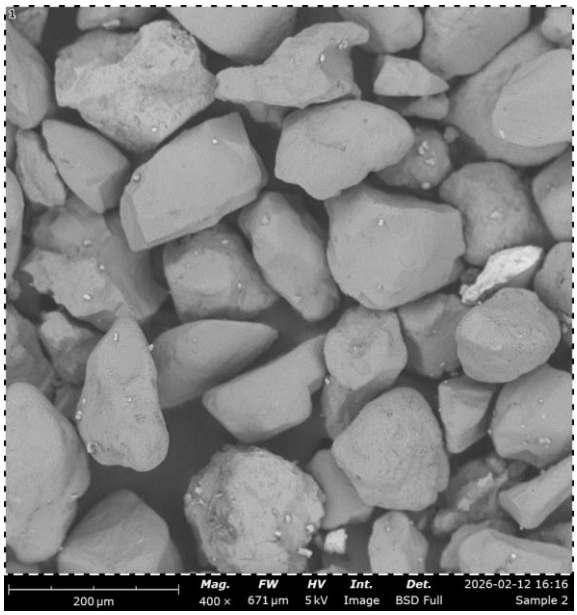

Element Number	Element Symbol	Element Name	Atomic Conc.	Weight Conc.
24	Cr	Chromium	95.80	93.12
38	Sr	Strontium	4.20	6.88

FOV: 671 µm, Mode: 5kV - Image, Detector: BSD Full, Time: FEB 12 2026 16:16

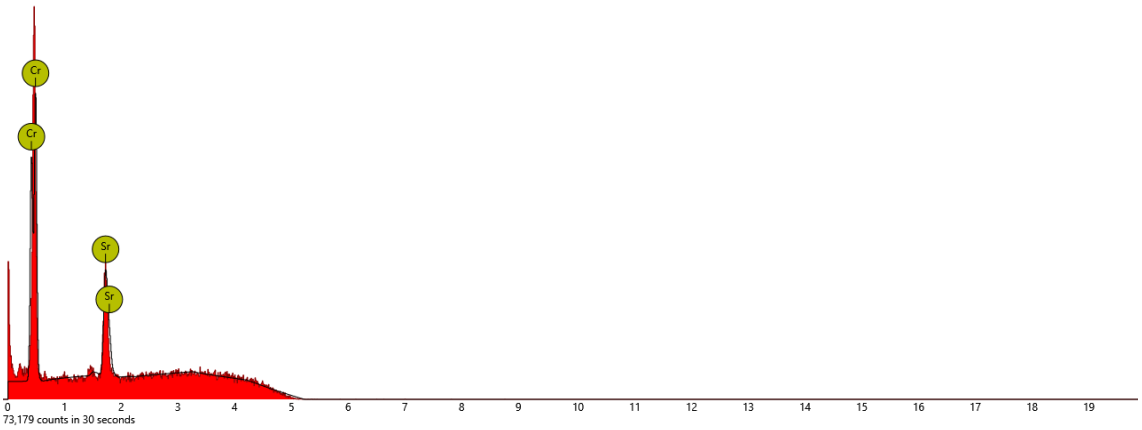

Disabled elements: B, O

International Journal of Engineering Research & Technology (IJERT)
ISSN: 2278-0181
Vol. 15 Issue 07 , July - 2026

E EDX

1. region

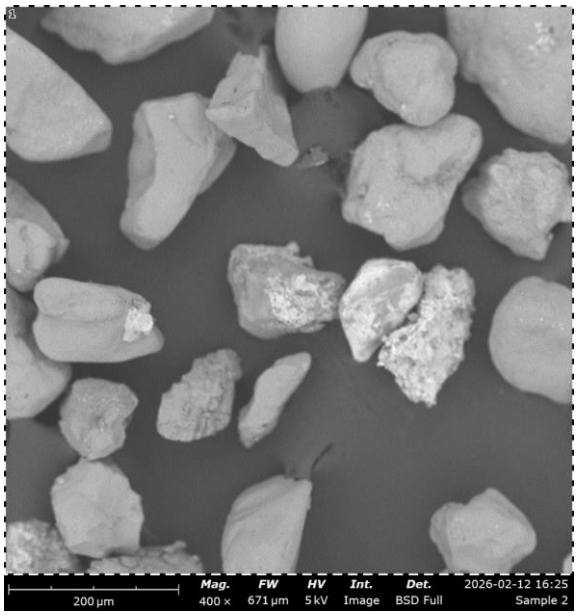

Element Number	Element Symbol	Element Name	Atomic Conc.	Weight Conc.
24	Cr	Chromium	95.48	94.60
38	Sr	Strontium	3.03	5.06

FOV: 671 µm, Mode: 5kV - Image, Detector: BSD Full, Time: FEB 12 2026 16:25

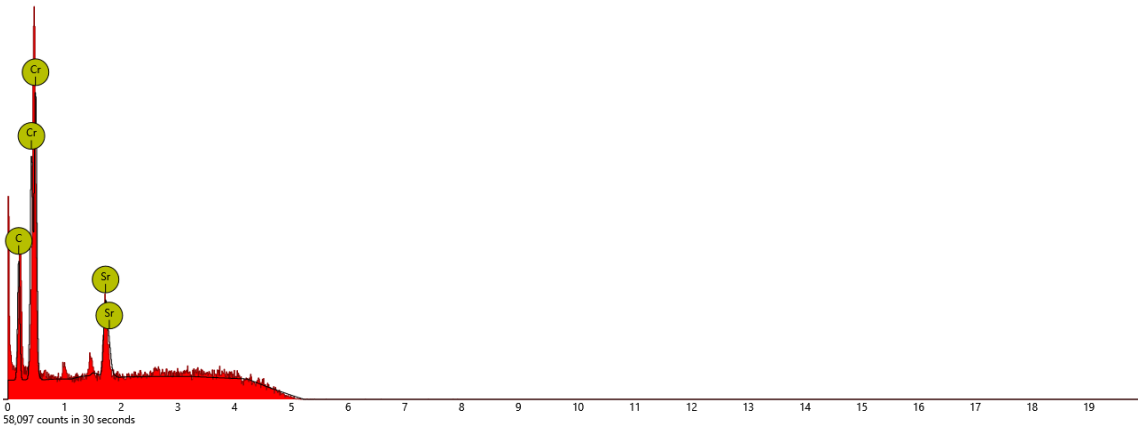

Disabled elements: B, O

3.4.1 Observed Elemental Composition

The EDX results for Samples A–E report the following elemental composition:

Sample	Chromium (Cr) wt.%	Strontium (Sr) wt.%
A	93.42	6.58
B	93.31	6.69
C	92.73	7.27
D	93.12	6.88

International Journal of Engineering Research & Technology (IJERT)
ISSN: 2278-0181
Vol. 15 Issue 07 , July - 2026

Sample	Chromium (Cr) wt.%	Strontium (Sr) wt.%
E	94.60	5.06

3.4.2 Interpretation of the EDX Results

The quantitative EDX report shows chromium (Cr) and strontium (Sr) as the dominant detected elements. However, this result is **not consistent** with the SEM observations or the XRF analysis performed on the same Wudil River sand.

The XRF analysis previously showed that the sand consists predominantly of silicon dioxide (SiO_2, approximately 76–80 wt.%), with smaller amounts of Al_2O_3, Fe_2O_3, K_2O, CaO, and TiO_2. Likewise, the SEM images clearly display quartz-rich sand grains that are characteristic of silica sand rather than chromium-bearing minerals.

A critical note in the EDX report states that oxygen (O) was disabled during the measurement. Oxygen is one of the principal constituents of silica (SiO_2), and excluding it from the analysis prevents the instrument from correctly quantifying silica. Furthermore, silicon (Si) is absent from the reported elemental table, despite quartz being the dominant mineral identified by XRF and SEM. This strongly suggests that the EDX acquisition or processing settings were incorrect, or that the elemental library/calibration used during analysis did not include the appropriate elements.

Consequently, the reported chromium- and strontium-rich composition should not be interpreted as representing the true bulk chemistry of the Wudil River sand.

3.4.3 Correlation with SEM Morphology

The SEM micrographs show predominantly quartz grains with sub-angular to sub-rounded morphology, smooth surfaces, and only localized roughness due to surface coatings and minor impurities. There is no evidence of extensive chromium-rich mineral phases that would justify chromium concentrations exceeding 90 wt.%. Similarly, only a few brighter particles were observed in the backscattered electron images, indicating the presence of small amounts of heavier minerals. If chromium- or strontium-rich minerals were truly dominant, the SEM images would be expected to show a much larger proportion of high-atomic-number phases with stronger backscattered electron contrast. Therefore, the SEM observations support the XRF results rather than the numerical EDX output.

3.4.4 Relationship with the XRF Analysis

The XRF analysis provides a more reliable representation of the overall chemical composition because it analyses the bulk sample rather than a very small localized region. The XRF results demonstrated that:

- SiO_2 is the major constituent (approximately 76–80 wt.%),
- Fe_2O_3 occurs at relatively low concentrations,
- Al_2O_3, K_2O, CaO, and TiO_2 are present as moderate impurities, and
- trace oxides occur only in small quantities.

These results agree well with the geological origin of river sand and with the observed SEM morphology. By contrast, the EDX results reporting chromium and strontium as the only major detected elements are inconsistent with both the mineralogical appearance of the particles and the XRF chemical composition. Accordingly, the XRF data should be regarded as the primary source for discussing silica extraction from the Wudil River sand.

3.4.5 Implications for Silica Extraction

Despite the limitations of the reported EDX dataset, the combined SEM and XRF results indicate that Wudil River sand remains a suitable source of silica. The SEM images show quartz grains with

International Journal of Engineering Research & Technology (IJERT)
ISSN: 2278-0181
Vol. 15 Issue 07 , July - 2026

relatively clean surfaces, while the XRF analysis confirms silica as the dominant component. The localized surface impurities observed by SEM are likely associated with iron oxides, aluminosilicates, feldspars, and titanium-bearing minerals rather than chromium-rich phases. These impurities can be removed effectively through:

- washing,
- attrition scrubbing,
- sieving,
- magnetic separation, and
- acid leaching.

Following beneficiation, the silica purity can be significantly increased, making the material suitable for industrial applications.

3.4.6 Relevance to PVC Solar Panel Development

For the manufacture of PVC solar panels, silica is used as a reinforcing filler to improve the mechanical, thermal, and weathering performance of the polymer composite. The suitability of Wudil River sand for this application is supported primarily by the SEM morphology and XRF chemistry, which indicate quartz-rich particles that can be purified to high-grade silica. Although the submitted EDX report does not provide a reliable elemental composition for silica because oxygen was disabled and silicon was not reported, the overall characterization demonstrates that the sand contains abundant quartz with removable surface impurities. After purification, the extracted silica is expected to:

- improve the tensile and flexural strength of PVC composites,
- enhance thermal stability,
- increase ultraviolet (UV) resistance,
- improve dimensional stability,
- reduce moisture uptake, and
- extend the service life of PVC solar panel components exposed to outdoor environments.

CONCLUSION.

The sieve analysis indicates that Samples C and D possess the most favorable particle size distributions for silica extraction because their medium-sized particles provide greater surface area for washing, impurity removal, and chemical purification. Samples A and E are dominated by coarse particles retained on the 600 µm sieve and would require additional crushing and milling, increasing processing costs. Sample B shows intermediate characteristics and could also be processed effectively.

However, particle size alone does not determine suitability for PVC solar panel manufacturing. The sand must also exhibit high silica (SiO_2) content, low iron (Fe_2O_3), and minimal clay, feldspar, and other contaminants. Consequently, the sieve analysis should be complemented by XRF/XRD and chemical purification studies before selecting the most appropriate sand source for manufacturing high-quality PVC solar panel materials.

The XRF analysis confirms that Wudil River sand is a viable source of silica for the production of PVC solar panel materials. Although the natural SiO_2 content (75.92–79.60 wt.%) is lower than the purity required for industrial-grade silica, the relatively low concentrations of iron and other trace impurities indicate that the sand can be upgraded through washing, magnetic separation, sieving, and acid leaching. Based on the chemical composition, Sample A is the most promising because of its highest silica content, while Sample D is also highly suitable due to its lower iron and titanium contents, which would reduce purification requirements and improve the quality of the extracted silica for PVC solar panel manufacturing.

International Journal of Engineering Research & Technology (IJERT)
ISSN: 2278-0181
Vol. 15 Issue 07 , July - 2026

The SEM analysis demonstrates that the Wudil River sand is composed predominantly of quartz grains with sub-angular to sub-rounded morphology, relatively smooth surfaces, minor surface roughness, and limited impurity coatings. The particles show favourable characteristics for beneficiation because impurities are mainly located on the grain surfaces rather than within the quartz matrix. These morphological features, together with the XRF results showing silica as the dominant oxide and the sieve analysis indicating suitable particle size distribution, confirm that the Wudil River sand is a promising raw material for the extraction of high-purity silica. Following appropriate beneficiation and purification processes, the extracted silica would be suitable as a reinforcing filler in PVC composites for solar panel applications, where it can improve the mechanical strength, thermal stability, weather resistance, and long-term durability of the final product.

The submitted EDX report identifies chromium and strontium as the detected elements in all five analysed regions; however, these results are inconsistent with the accompanying SEM observations and the XRF analysis of the same Wudil River sand. Because oxygen was disabled during the EDX acquisition and silicon is absent from the reported elemental tables, the quantitative EDX results should not be used as the principal evidence for evaluating silica extraction. Instead, the XRF and SEM analyses provide a more reliable characterization, demonstrating that the Wudil River sand is predominantly quartz with moderate surface impurities that can be removed through beneficiation and acid leaching. Therefore, the sand remains a promising raw material for producing high-purity silica suitable for use as a reinforcing filler in PVC solar panel manufacturing.

Recommendation:

It is recommended to verify the instrument settings and repeat the EDX analysis with silicon (Si) and oxygen (O**)** enabled. A correct EDX spectrum for silica sand should show strong Si and O peaks, with only minor peaks for impurities such as Fe, Al, Ti, Ca, K, and other trace elements. This would provide results that are consistent with both the SEM morphology and the XRF chemical composition.

Acknowledgement.

The author wishes to acknowledge to the management of Kano State Polytechnic, and Colloquies at Welding and Fabrication Department more especially Material Science Laboratory, Chemistry Laboratory Technologist for guidance and assistance during pre-treatment of the sand sample and general use of laboratory facilities.

Funding.

The research was funded by tertiary education trust fund (TETfund) with grand allocation number TETF/DR&D/CE/POLY/KANO/RG/2025/VOL.1

REFERENCES

[1] International Energy Agency, *Renewables 2023: Analysis and Forecast to 2028*. Paris, France: IEA, 2023.
[2] International Renewable Energy Agency, *Renewable Capacity Statistics 2024*. Abu Dhabi, UAE: IRENA, 2024.
[3] International Energy Agency, *World Energy Outlook 2023*. Paris, France: IEA, 2023.
[4] Fraunhofer Institute for Solar Energy Systems, *Photovoltaics Report*, 2024.
[5] Martin A. Green, Emery K. Dunlop, Jochen Hohl-Ebinger, Masahiro Yoshita, and Xiaojing Hao, "Solar cell efficiency tables (Version 64)," *Progress in Photovoltaics: Research and Applications*, vol. 32, no. 7, pp. 425–438, 2024.
[6] United States Geological Survey, *Mineral Commodity Summaries 2024: Silicon*. Reston, VA, USA: U.S. Geological Survey, 2024.
[7] Silicon Processing for the VLSI Era, vol. 1. Sunset Beach, CA, USA: Lattice Press, 2018.
[8] M. I. Ojovan and W. E. Lee, *An Introduction to Nuclear Waste Immobilisation*, 3rd ed. Amsterdam, Netherlands: Elsevier, 2019.
[9] John D. Cressler and H. A. Mantooth, *Extreme Environment Electronics*. Boca Raton, FL, USA: CRC Press, 2017.
[10] R. Hou, Y. Li, and X. Wang, "Purification and characterization of quartz sand for high-purity silica production," *Minerals Engineering*, vol. 145, Art. no. 106091, 2020.
[11] B. A. Wills and James Finch, *Wills' Mineral Processing Technology: An Introduction to the Practical Aspects of Ore Treatment and Mineral Recovery*, 9th ed. Oxford, U.K.: Butterworth-Heinemann, 2023.
[12] M. Vegliò, F. Beolchini, and L. Toro, "Acid leaching optimization for silica purification: A review," *Hydrometallurgy*, vol. 214, Art. no. 105968, 2022.
[13] J. Goldstein, D. Newbury, P. Echlin *et al.*, *Scanning Electron Microscopy and X-ray Microanalysis*, 4th ed. New York, NY, USA: Springer, 2018.
[14] R. Jenkins and R. Snyder, *Introduction to X-ray Powder Diffractometry*. New York, NY, USA: Wiley, 2019.
[15] ASTM International, *ASTM C136/C136M-19: Standard Test Method for Sieve Analysis of Fine and Coarse Aggregates*. West Conshohocken, PA, USA: ASTM International, 2019.

International Journal of Engineering Research & Technology (IJERT)
ISSN: 2278-0181
Vol. 15 Issue 07 , July - 2026

[16] Nigerian Geological Survey Agency, *Geological Map and Mineral Resources of Nigeria*. Abuja, Nigeria: NGSA, 2022.
[17] Raw Materials Research and Development Council, *Report on Industrial Minerals in Nigeria*. Abuja, Nigeria: RMRDC, 2021.
[18] Federal Ministry of Science, Technology and Innovation, *National Policy on Science, Technology and Innovation*. Abuja, Nigeria, 2022.
[19] A. Luque and Steven Hegedus, *Handbook of Photovoltaic Science and Engineering*, 3rd ed. Hoboken, NJ, USA: Wiley, 2021.
[20] M. A. Green, "Commercial progress and challenges in crystalline silicon photovoltaics," *Nature Energy*, vol. 6, no. 8, pp. 761–772, 2021.
[21] P. Swarnkar, S. Khan, and R. Singh, "Beneficiation of silica sand for glass and photovoltaic applications: A review," *Minerals Engineering*, vol. 183, Art. no. 107604, 2022.
[22] A. Mehdilo, M. Irannajad, and A. Rezai, "Optimization of acid leaching parameters for purification of silica sands," *Separation Science and Technology*, vol. 56, no. 14, pp. 2451–2464, 2021.
[23] N. A. Adekoya, A. S. Adekunle, and O. O. Borode, "Purification of quartz using mixed-acid leaching techniques for high-purity silica production," *Journal of Materials Research and Technology*, vol. 15, pp. 3765–3778, 2021.
[24] R. Jenkins, *X-ray Fluorescence Spectrometry*, 2nd ed. New York, NY, USA: Wiley, 2019.
[25] Joseph Goldstein, Dale Newbury, David Joy, *et al.*, *Scanning Electron Microscopy and X-ray Microanalysis*, 4th ed. New York, NY, USA: Springer, 2018.
[26] D. B. Williams and C. Barry Carter, *Transmission Electron Microscopy: A Textbook for Materials Science*, 2nd ed. New York, NY, USA: Springer, 2016.
[27] ASTM International, *ASTM E11-22: Standard Specification for Woven Wire Test Sieve Cloth and Test Sieves*. West Conshohocken, PA, USA: ASTM International, 2022.
[28] L. Nicolais and Gianfranco Carotenuto, *Metal-Polymer Nanocomposites*. Hoboken, NJ, USA: Wiley, 2019.
[29] M. Xanthos, *Functional Fillers for Plastics*, 3rd ed. Weinheim, Germany: Wiley-VCH, 2020.
[30] A. A. Elueze and M. A. Bolarinwa, "Industrial silica sand deposits and their economic potential in Nigeria," *Journal of African Earth Sciences*, vol. 184, Art. no. 104356, 2021.
[31] A. A. Hassan, S. Ibrahim, and M. U. Garba, "Characterization of silica-rich river sand deposits from northern Nigeria for industrial applications," *SN Applied Sciences*, vol. 4, no. 5, Art. no. 151, 2022.
[32] A. A. Adebayo, O. O. Adewuyi, and K. O. Olalekan, "Evaluation of silica sand deposits for photovoltaic-grade silicon production," *Materials Today: Proceedings*, vol. 49, pp. 2864–2871, 2022.